Ultrasonics Sonochemistry 107 (2024) 106925

Contents lists available at ScienceDirect

Ultrasonics Sonochemistry

journal homepage: www.elsevier.com/locate/ultson

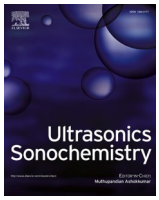

Ultrasonic reactor set-ups and applications: A review

Panayiota Adamou [a,1], Eleana Harkou [a,1], Alberto Villa [b], Achilleas Constantinou [a,*], Nikolaos Dimitratos [c,d,*]

[a] Department of Chemical Engineering Cyprus University of Technology, 57 Corner of Athinon and Anexartisias, 3036 Limassol, Cyprus
[b] Dipartimento di Chimica, Universitá degli Studi di Milano, via Golgi, 20133 Milan, Italy
[c] Department of Industrial Chemistry "Toso Montanari", University of Bologna, viale Risorgimento 4, 40136 Bologna, Italy
[d] Center for Chemical Catalysis – C3, University of Bologna, viale Risorgimento 4, 40136 Bologna, Italy

ARTICLE INFO

Keywords:
Sonochemistry
Microstructured sonoreactors
Operational parameters
Applications
Challenges
Perspectives

ABSTRACT

Sonochemistry contributes to green science as it uses less hazardous solvents and methods to carry out a reaction. In this review, different reactor designs are discussed in detail providing the necessary knowledge for implementing various processes. The main characteristics of ultrasonic batch systems are their low cost and enhanced mixing; however, they still have immense drawbacks such as their scalability. Continuous flow reactors offer enhanced production yields as the limited cognition which governs the design of these sonoreactors, renders them unusable in industry. In addition, microstructured sonoreactors show improved heat and mass transfer phenomena due to their small size but suffer though from clogging. The optimisation of various conditions of regulations, such as temperature, frequency of ultrasound, intensity of irradiation, sonication time, pressure amplitude and reactor design, it is also discussed to maximise the production rates and yields of reactions taking place in sonoreactors. The optimisation of operating parameters and the selection of the reactor system must be considered to each application's requirements. A plethora of different applications that ultrasound waves can be implemented are in the biochemical and petrochemical engineering, the chemical synthesis of materials, the crystallisation of organic and inorganic substances, the wastewater treatment, the extraction processes and in medicine. Sonochemistry must overcome challenges that consider the scalability of processes and its embodiment into commercial applications, through extensive studies for understanding the designs and the development of computational tools to implement timesaving and efficient theoretical studies.

1. Introduction

Sonochemistry involves the implementation of sonic and ultrasonic waves where the molecules bear a chemical reaction to contribute to the green chemistry's goals by implementing more environment-friendly methods to overcome the environmental crisis which becomes more evident every year. Sound waves greater than 20 kHz are considered as ultrasonic sound and ultrasound and can be divided into three major categories, low, intermediate, and high frequency. Acoustic cavitation is regarded as the driving force which produces supreme temperatures and pressures. The chemical reactions and strong physical forces that occurred are due to the interaction between the ultrasound and the bubbles in liquids and can be utilised in various applications promoting chemical reactions in waste treatment, in medicine, for the synthesis of nanoparticles and in analytical chemistry [1,2]. Shortener reaction times and higher selectivity and yields than the conventional heating are some of the benefits ultrasonic waves offer [3].

The system in which the sonochemical reactions occur is generically a multi-bubble environment where virtually the chemical reactions occur in connection with the strongly and rapidly compressed and heated interior of collapsing bubbles [4]. Due to the violent collapse of cavities in the liquid and the large magnitudes of energy released, sonochemical reactors are used to perform multiphase reactions at laboratory- and pilot-scale capacity [5]. A wide range of recent review papers exists providing overviews either for the materials and the characteristics of sonochemical reactions and mechanisms, or for the reactor design and the operating parameters [1,5–8]. Moreover, applications of sonochemical reactions focus on the wastewater treatment and environmental applications [9–13]. This is an up-to-date work collecting all the knowledge that needs to be considered for the

* Corresponding authors.
E-mail addresses: a.konstantinou@cut.ac.cy (A. Constantinou), nikolaos.dimitratos@unibo.it (N. Dimitratos).
[1] These authors share first authorship.

https://doi.org/10.1016/j.ultsonch.2024.106925
Received 26 January 2024; Received in revised form 1 May 2024; Accepted 22 May 2024
Available online 26 May 2024

development and design of sonochemistry processes considering all the phenomena occurring inside the sonoreactors. This review aims to present the different sonochemical reactor designs that are specific for each application to maximize the activity and yields of cavitation and discuss the advantages and disadvantages of each reactor design. In addition, primary and secondary regulation conditions, including the temperature, the frequency of ultrasound, the intensity of irradiation, the pressure of amplitude, the sonication time and the geometry and the construction material of the reactor, are discussed for the successful optimisation for achieving the maximum benefits and also it is provided an overview of various applications in which the sonochemical reactors were used efficiently.

2. Theoretical background

The formation, growth and violent collapse generated by sound waves is referred to the acoustic cavitation. Through the rarefaction pressure cycle the bubbles expand while in the compression pressure cycle they shrink [14]. When the ultrasound intensity is significant to conquer medium's tensile strength, a point exists where the intermolecular forces cannot hold the molecular structure together and the cavity is formed in the medium. The formation of bubbles occurs through various different mechanisms such as the gas molecules that are captured in crevices of the container walls, motes or on hydrophobic dust particles, the skin model where inherently present bubble nuclei are stabilised against dissolution when their surface is completely covered with organic materials or surfactants and the fragmentation of the active cavitation bubbles [1].

The bubbles contain vaporised gas or liquid that was formerly liquified in a medium. They get bigger in size throughout the oscillations and as they reach a sonorousness size they violently cave in or implode during the wave compression part (Fig. 1) [15]. Extreme pressures and temperatures are formed with the collapse of bubbles that highly reactive redox radicals are formed and are used to initiate chemical reactions [14]. In a few words, diffused ultrasonic energy is concentrated within the hot spots which can be considered as microreactors creating regions inside the bubble, at the bubble–liquid interface and in the liquid bulk for high-energy chemical reaction.

Li et al. [16], used the cavitation mechanism to validate experimental results of a fixed geometry oil film journal bearing using the Reynolds equation algorithm. The oil film bearing cavitation mechanism was attributed to gaseous cavitation and the model was designed based on air solubility in the lubricant. The theoretical results could describe the phenomena that take place in most of the cases excluding the very heavy oil-films. Moreover, the model was found to agree with the Jakobsson-Floberg-Olsson condition and can recall whether vaporous cavitation happens as well as innovative means for the development of cavitation models for low-vapor-pressure lubricants.

Xu et al. [17], carried out an investigation in a jet pump cavitation reactors (JPCRs), of the cavitation initiation characteristics and mechanisms to strengthen the cavitation. A criterion obtained for cavitation initiation focuses on the fluctuating pressures generated by the gradients of velocity where experimental results showed that the criterion predicted strong shear dominant cavitation and low-pressure cavitation in the JPCR. The gradient of velocity and the coefficient loss were found to be raised with the reduction of suction pressure promoting the cavitation. In addition, it was observed that at the evolution of the low-pressure cavitation, the low-frequency component was dominant while the high frequency component dominated at the strong shear dominant cavitation formation.

3. Sonochemical reactors set-ups

3.1. Features

A typical ultrasonic system consists of a generator, one or more transducers, and depending on the application, a booster and an emitter [18]. The ultrasonic generator generates an electrical current with a predetermined power rating and the transducer, in response to the excitation signal provided by the generator, converts the energy into ultrasonic vibrations [19]. The emitter is used to increase the amplitude of ultrasonic vibrations generated by the transducer and transfer the ultrasonic wave into the medium, while the booster alters further the amplitude before they reach the horn [20]. Fig. 2 depicts all the features that an ultrasonic system might consist of. Up to a transducer is a complete system and the booster and probe can be added depending on the process. Details of these components are discussed in the following section.

3.1.1. Ultrasonic generators

For an effective sonication, the ultrasonic generator is a key aspect. In more detail, enough amplitude in the horn can only be produced with a high drive voltage delivered to the transducer. Consequently, the ultrasonic generator transforms the input power supply at high adjustable frequencies to energize the transducer for it to generate ultrasonic vibration as a result of the excitation signals. If the generator has a poor performance, then the whole process is insufficient. The generator is categorised into two modes: the self-excited and the other-excited power supply. The former needs manual adjustment and can easily be detuned and operate at a non-resonant state. Thus, the ultrasonic vibration is

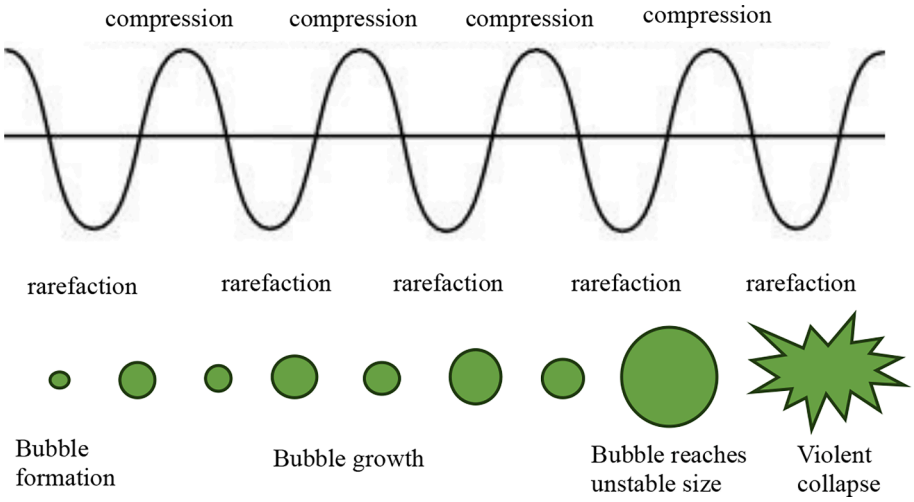

Fig. 1. Formation of acoustic bubble.

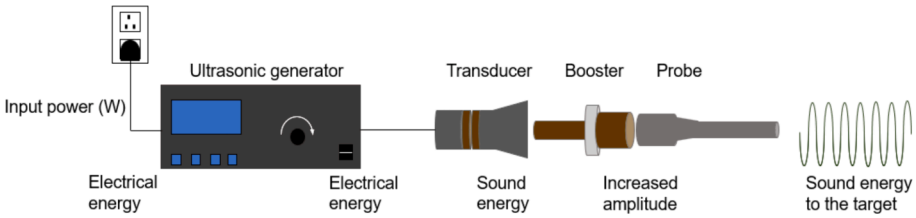

Fig. 2. Schematic representation of all possible ultrasonic features [18–20].

reduced, and the output is mainly converted to heat and hence, it is not much used anymore. The other mode is a closed-loop system that can automatically adjust the output frequency for the transducer to operate at the resonance point [18]. Up to this point, generators do not quickly and accurately respond to the frequency shift caused by the thermo-mechanical load, high temperature, and other parameters [21].

3.1.2. Transducers

Transducers can convert electrical energy to mechanical energy, generating ultrasound waves resulting in acoustic cavitation. The transducers can be attached on the bottom on the outer sidewall of the reactor or they can be directly immersed in the solution [22]. The intensity of the sound attenuates as the distance of the transducer increases, affecting the acoustic cavitation and contributing to the presence of active and passive zones. When an oscillating force occurs at a frequency very close to the transducers "natural" frequency then the transducer works under a resonant state, maximising the efficiency [18]. They are usually made from piezoelectric materials that can generate electric voltage when are placed upon mechanical stress.

3.1.2.1. Plate transducers. A plate transducer can be attached to the bottom of the outside of the reactor. They usually operate at a range of 0–200 W of electric power and a frequency of 20 kHz-5 MHz [23]. This type of transducer is very common and even utilised in larger-scale applications. However, there is a major disadvantage: the liquid height in the vessel. Since the acoustic field is irradiated only from the bottom, a big height of the liquid will result in the formation of hot spots near the liquid surface, far from the plate. Therefore, the liquid height is a crucial parameter.

3.1.2.2. Ultrasonic submersible transducers. The transducers can also be in direct contact with the medium for sonication by submerging them in the reactor instead of attaching them to the outer surface. They can be placed in the tank's side, bottom or top. Compared to conventional systems described above in Section 3.1.2.1, the submersible transducers offer many advantages. Firstly, their position can be controlled to enhance the cavitation and they can work under the frequency range of 20–132 kHz altering it based on the application used. They are extensively used in the food industry and for cleaning because they have higher efficiency due to the direct exposure of ultrasound in the solution. Introducing another ultrasonic transducer in a system with a submersible transducer create a multi-frequency ultrasonic tank resulting in even higher efficiency [24].

3.1.2.3. Langevin-type transducer. When high ultrasonic powers and low frequencies are required, the Langevin transducer is mostly used. Two piezoelectric ceramic plates are clamped among two metal masses protecting the ceramic and preventing it from overheating. Typically, the metal used for the front mass is lighter than that of the back mass and thus, the soundwave is mostly irradiated from the front and occasionally with the help of an ultrasonic probe to guide the ultrasonic waves [25]. A schematic representation of a Langevin transducer is shown below (Fig. 3) [26]. As it can be seen the front mass is in conic shape since it is the output of the transducer. A bolt is attached at the bottom, bracing the whole system and applying compression, increasing the vibrational

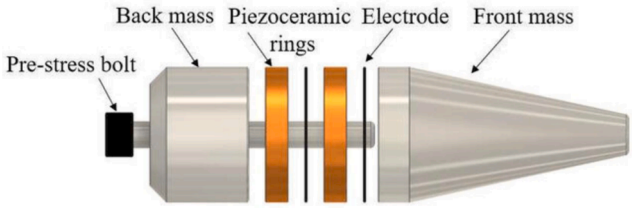

Fig. 3. Schematic structure of the Langevin-Type Transducer [26].

movement of the plates [27].

3.1.3. Ultrasonic horn

Ultrasonic horn or ultrasonic probe or sonotrode is directly submerged in a solution, transmitting soundwaves to the target. The horn can be attached at the end of the transducer, and they are usually used when high intensity is required. Ultrasonic waves with a frequency of 20–30 kHz, are transmitted from the transducer to the horn tip where very high intensities are detected [20]. However, depending on the equipment's maximum power input and the operating frequency, the intensity decreases dramatically while increasing the distance from the horn.

The horn can send both standing and travelling waves, but travelling soundwaves are the dominant in the system resulting in better acoustic cavitation [28]. Since the sonotrode is immersed in the medium, the material is an important parameter to consider for each application. They must be characterised by great acoustic properties and good resistance from corrosion and heat. The most common materials are titanium alloy, aluminium, and stainless steel [29].

3.1.4. Booster

An ultrasonic booster is not a mandatory part of an ultrasonic system. It is also known as amplifier since it increases the amplitude of ultrasonic vibrations of the transducer and passes them to the sonotrode [30]. It is installed between the transducer and the horn providing also rigid support to the ultrasonic assembly. Usually, the diameter of the booster at the end of the booster that is attached to the probe is small to ensure the increased amplitude that is transmitted to the probe.

Seeing that it affects the vibrations that a transducer sends to the probe, it is important to take into account the amplitude and resonant frequency when designing a booster. Furthermore, the impact of temperature needs to be considered. The temperature is increasing at the nodes of the booster, during ultrasonic vibration, altering density and elastic modulus values of the material, causing the resonant frequency of the ultrasonic booster to decrease [18].

3.2. Reactors

Reactor configuration has an essential role regarding the cavitation activity. The nature of cavitation activity is non-homogeneous. This means that there are dead zones in sonochemical reactors in addition to active cavitation zones. Thus, the reactor configuration can affect how the active and dead zones are distributed as well as the overall volume that is cavitationally active. The latter is essential to ultrasonic

attenuation, which is the reduction in pressure intensity with increasing distance from the transducer, affecting the intensity of cavitation in different places.

Batch and continuous reactors are the two main categories of sonoreactors. There are significant variations, as seen in Fig. 4, regarding the reactor design such as dimensions, flow parameters, direct or indirect sonication method, number and type of transducer, the ratio between the vessel and the transducer and reactor geometry. Table 1 summarises different reactor configurations utilised for various sonochemical applications.

3.2.1. *Ultrasonic batch systems*

Batch reactor systems are widely used due to their low cost, small and simple set-up (0.03 L- 130 L). Nevertheless, they are usually used for small-scale production, approximately in the range of $2x10^{-6}$ – $20x10^{-10}$ mol/J (the yield is given in sonochemical efficiency – molecules reacted to the ultrasound energy) [59]. In the case of ultrasound reactor systems, a large amount of research was focused on conventional systems such as batch reactors [60]. The application of ultrasound combined with a batch system, enhances the mixing thus, the mass transfer phenomena and reaction rates in multiple biological/chemical processes. However, the acoustic fields that are generated via ultrasound, fades swiftly with the spreading distance and therefore nearly all of the energy is transformed to thermal energy, resulting in low efficiency of acoustic energy making it difficult to control and scale. To escalate the field of sound pressure and cavitation, it is necessary to optimise the geometry of the device [61].Thus, one of the most crucial factors affecting acoustic cavitation in batch systems is the vessel's liquid height [6].

The most used ultrasonic equipment in batch systems is the ultrasonic bath, the sonotrode and the cup-horn as discussed below. In simpler systems, a single transducer can be used as an ultrasonic source in a beaker or a bath. Each one of this equipment affects the acoustic field and thus the efficiency of the process. Son et al. [31], studied the energy distributions of acoustic cavitation at different frequencies in a large-scale reactor. The reactor was made up of an ultrasonic transducer module positioned in the centre of an acrylic bath. The best cavitation energy distribution in terms of stability was found at 72 kHz. Nonetheless, the difference in half-cavitation-energy distance between a lower frequency (35 kHz) and 72 kHz, showed that the cavitation energy for a single cycle was greater at the lower frequency. Furthermore, the cavitation energy distribution was extremely low and poor for higher frequency. Additionally, it was discovered that cavitations energies ranging from 31.76 to 103.67 W could generate a sonochemical efficiency from $7.77x10^{-10}$ to $4.42x10^{-10}$ mol/J. Lastly, a quadratic relationship was found between sonochemical efficiency and cavitational energy.

In another study, Son et al., [62], examined the effect of the distance from the ultrasonic source on the sonochemical activity in 36 and 108 kHz cylindrical sonoreactors with different liquid heights (80 and 340 nm). The glass cylindrical column with a height of 500 mm and a diameter of 110 mm, contained one PZT ultrasonic transducer at the bottom generating 36 and 108 kHz frequencies. When the same input energy was used, the cavitation yield was highly increased as the liquid height/irradiation distance increased. Higher liquid heights resulted in the formation of a stronger and more stable standing wavefield. Based on these results, the authors concluded that, one of the key design elements for large-scale sonoreactors to maximise the sonochemical activity might be the optimisation of the ultrasonic irradiation distance.

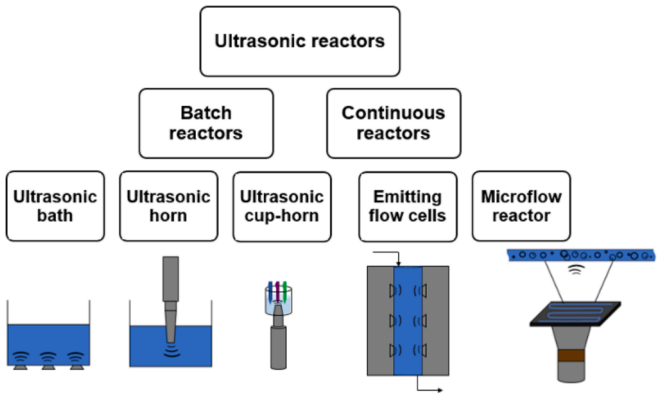

Fig. 4. Types of ultrasonic reactors and ultrasonic equipment used for each type.

A study by Lim et al. [33], showed the effects of varying liquid height/volumes and input powers on sonochemical oxidation reactions, including iodide ion oxidation, As(III) oxidation, and hydrogen peroxide generation. A glass cylindrical column housed a 291 kHz ultrasonic transducer which served as the sonoreactor for this study, similar to the set-up described above. Varying the power density from 23 to 1640 W/L, the greatest cavitation yields of triiodide ions at 23, 40 and 82 W were reported at 0.05, 0.1 and 0.2–0.3 L respectively. Moreover, low power was more efficient for small volumes, while high power levels were needed for big volumes. A moderate power density of 400 W/L was recommended for the sonochemical oxidation of iodide ions in the 291 kHz sonoreactor. Analogous outcomes were observed for the hydrogen peroxide production and the As(III) oxidation.

Using a novel Langevin-type transducer, operating at 20 kHz, the impact of liquid height on the mechanical and chemical effects was investigated by Tran et al. [34]. The degradation of an aqueous solution of polyethylene oxide was used to assess the mechanical impacts, while a potassium iodide solution was used to measure the chemical effects. Using aluminum foil erosion and sonochemical luminescence, standing waves or reactive zones were detected. Mechanical effects were decreased at higher liquid heights, while chemical effects were stable after 120 mm. When compared to conventional transducers, the mechanical and chemical effects of the transducer studied were significantly enhanced due to its better structure.

A cylindrical reactor's sonochemical efficiency was studied in relation to frequency and liquid height by Asakura et al. [35]. Liquid height was ranging from 10 to 700 mm and irradiation frequency from 45 to 490 kHz. A cylindrical acrylic pipe was used as the sonoreactor with a stainless steel vibration plate at the base, below a transducer driven by a high- or low-frequency power amplifiers. Sonochemical efficiency was influenced by both frequency and liquid height and the plots of sonochemical efficiency vs liquid height exhibited one or two peaks for every frequency. Up until the first peak, the sonochemical efficiency rose monotonically with the frequency logarithm, and the liquid height for the first peak had an inverse relationship with frequency. Another study by Asakura et al. [36], focused on the optimisation of sonochemical processes by focusing on acoustic features of the cylindrical sonochemical reactor described above. Results demonstrated efficiency peaks when impedance was minimised, particularly at liquid heights corresponding to resonance conditions. Transducer impedance and sonochemical efficiency were highly influenced by the reactor's upper-end configuration-fixed or free end. Lastly, when the harmonies components were increased and the subharmonics decreased, higher sonochemical efficiency was attained.

Kobayashi et al. [37], studied the effects of the reactor's positioning on chemical and physical degradation, and emulsion polymerisation of styrene under indirect ultrasonic irradiation. The experiments were conducted in a water bath, housing a glass reactor and seven transducers. The placement of the reactor affected the molecular weight and polymer yield. The shock wave index derived from literature and the extent radical generation, measured by the KI oxidation dosimetry, were helpful in regulating the properties of the polymer produced. Additionally, the effect of irradiation distance and ultrasonic power on radical generation was also investigated [38], for the degradation of phenol using a similar set-up. A simple kinetic model revealed a linear correlation among the ultrasonic power and the rate constant of phenol

Table 1
Reactor set-ups used for ultrasound-assisted applications.

Reactor	Design characteristics	Experimental conditions	Process	Yield/Target	Ref.
Batch	Acrylic large-scale sonoreactor (120 × 60 × 40 cm), nine PZT transducers (20 × 20 × 7 cm)	35, 72, 110, 170 kHz, 240 W, 18–19 °C	Distribution of acoustic cavitation energy	–	[31]
Batch	Glass cylindrical column, one PZT transducer	36, 108 kHz	Effect of distance from the ultrasonic source on the sonochemical activity	–	[32]
Batch	Glass cylindrical column, one transducer	291 kHz, 20 °C	Liquid height/volume effect, input acoustic power effect	–	[33]
Batch	Stainless steel sonoreactor, Langevin transducer	19.8 kHz, 25 ± 1 °C	Impact of the liquid height on mechanical and chemical effects	–	[34]
Batch	Cylindrical acrylic pipe reactor, stainless steel vibration plate at the bottom, transducer	45, 129, 231 and 490 kHz, 25 ± 2 °C	Effect of sonochemical efficiency in relation with frequency and liquid height	–	[35]
Batch	Acrylic pipe reactor, Langevin transducer	129 kHz, room temperature	Optimisation by focusing on acoustic features	–	[36]
Batch	Glass reactor in a water bath, seven transducers	28, 45, 100 kHz, 30, 50 °C	Effect of the reactor positioning on chemical and physical degradation	–	[37]
Batch	0.05 L glass reactor in a water bath, seven transducers	28 kHz, 300 W, 30 °C	Effects of irradiation distance on degradation of phenol	–	[38]
Batch	10 L reactor, multi-frequency transducer plates	700, 950 kHz	Scale-up of the sonolytic destruction of Per and Polyfluoroalkyl substance (PFAS)	–	[39]
Batch	Acrylic rectangular sonoreactor (13 × 13 × 30 cm), transducer module positioned at the bottom of the sonoreactor.	28 kHz	Effect of mixing rate on sonochemical oxidation activity under various liquid height/volume conditions.	–	[40]
Batch	2.7 L open rectangular ultrasonic cleaner bath with internal dimensions of 14 × 24 × 9 cm	25 kHz, 150 W, 30 °C	Sonoextraction from jaboticaba peels	4.8 mg/g monomeric anthocyanin, 92.8 mg/g gallic acid, 4.9 mg/g cyanidin-3-O-glucoside 7.8 mg/g ellagic acid	[41]
Batch	Bath-type sonoreactor (11 × 11 × 20 cm), plate type ultrasound transducer module with one PZT transducer (5 cm) at the bottom	291, 448 kHz	Effect of liquid height on different reactions	–	[42]
Batch	Bath-type sonoreactor (20 × 20 × 20 cm), plate type ultrasound transducer module with one PZT transducer (5 cm) at the bottom	291, 448 kHz	Effect of liquid height on different reactions	–	[42]
Batch	–	200 W, 50 °C	Synthesis of S-scheme heterojunction	95 % RhB removal	[43]
Batch	0.1 L×beaker, 13 mm diameter probe	20 kHz, 100 W/cm^2	Synthesis of $Cu_2O@TiO_2$ heterojunction nanocomposites	75 % MO removal	[44]
Batch	0.15 L flat bottom cylindrical glass beaker, 10 mm pitched blade impeller	50 kHz, 80 W	Crystallisation	350–400 μm crystal size	[45]
Batch	150 mL flat bottom cylindrical glass beaker, 2-cm diameter horn tip	36 kHz, 120 W	Crystallisation	200–250 μm crystal size	[45]
Batch	6 L ultrasonic bath with dimensions 350 × 120 × 200 mm, (transducer dimensions 200 × 50 mm), 0.5 L baffled rectangular Borosil glass reactor (8 × 13 cm)	20 kHz, 1 kW, 30–60 °C	Generation of biodiesel from mahua oil	55 %	[46]
Batch	Baffled rectangular glass reactor of 0.5 L capacity (8 × 13 cm), ultrasonic horn	20 kHz, 120 W, 30–60 °C	Generation of biodiesel from mahua oil	93 %	[46]
Batch	0.5 L circular glass vessel, 13 mm diameter threaded-end probe	20 kHz	Optimisation of geometric and operational parameters	–	[32]
Batch	Ultrasonic flat transducer probe immersed in glass cylinder sonoreactor	20 kHz	Investigation of water sonication	–	[47]
Batch	Glass cylindrical reactor (5 × 12 cm), cup horn of 76 mm diameter and 165 mm long	20 kHz, 750 W, 50 % amplitude, 30 °C	Conversion of lignocellulosic materials into furfural	72.4 ± 4.3 mg/g furfural	[48]
Batch	Glass cylindrical reactor (5 × 12 cm)	25–37 kHz, 100–330 W, 30–70 °C	Acid hydrolysis of cellulose	–	[49]
Batch	Glass cylindrical reactor (5 × 12 cm), titanium probe of 13 mm diameter and 254 mm long	20 kHz, 750 W, 50 % amplitude, 30–70 °C	Acid hydrolysis of cellulose	–	[49]
Batch	Glass cylindrical reactor (5 × 12 cm), cup horn of 76 mm diameter and 165 mm long	20 kHz, 750 W, 50 % amplitude, 30–70 °C	Acid hydrolysis of cellulose	78 %	[49]
Batch	Beake× immersed in a cup horn above a transducer of 5 cm	20 kHz, 750 W, 40 % amplitude, 25–34 °C	Synthesis of Bi_2WO_6 nanostructures	99.5 % RhB/MB removal	[50]
Continuous flow	Flow cell modified by a flow insert (8 mL available volume), ultrasonic horn	100 W, 85 °C	Synthesis of metastable CdS nanoplatelets	21 nm hexagonal CdS platelets	[51]
Batch	316 L stainless steel ultrasonic bath (34 L available capacity), glass reactor, 12 transducers	170 kHz, 25 °C	KI oxidation on aluminium erosion	–	[52]
Continuous flow	Flow-through ultrasonic reactor jacket, mixing tank (45 L total volume of the system)	170 kHz, 25 °C	KI oxidation on aluminium erosion	–	[52]
Continuous flow	Plexiglass tubular sonoreactor with two transducers	20 kHz, 48 W	Cracking and desulfurization of petroleum products	81 % sulphur removal	[53]

(*continued on next page*)

Table 1 (*continued*)

Reactor	Design characteristics	Experimental conditions	Process	Yield/Target	Ref.
Continuous flow	Flatbed reactor, reaction chamber of 100 × 8 × 4 cm with six external transducers	25 kHz, 300 W	Pre-treatment of waste activated sludge	170–260 mL CH_4/g_{vs} methane yield	[54]
Continuous flow	Flatbed reactor, reaction chamber of 100 × 8 × 4 cm with six external transducers	25 kHz, 300 W	Flow of water containing two sewage sludge substitutes	–	[55]
Batch	8 L reactor of 15 × 33 × 20 cm, 24 cm long horn	36 kHz, 150 W	Cavitational activity distribution	–	[56]
Continuous flow	7.5 L hexagonal flow cell, six transducers (6 cm diameter)	20,30,50 kHz, 150 W	Cavitational activity distribution	–	[56]
Microflow	Glass sonoreactor, 3 mm micro-tip ultrasonic probe	20 kHz, 200 W	Deposition of TiO_2 nanoparticles on a FEP microtube	TOF = 0.41 1/s of phenol degradation	[57]
Microflow	4 microchannels 100 μm x 50 mm, 65 mm diameter transducer	200 kHz	MO removal	9 % MO removal	[58]

degradation. Despite variations in sample volume and equipment, a linear relationship was observed between the degradation rate constant and ultrasonic energy within the 20–30 kHz frequency range, contrasting the significantly higher degradation rate within the range of 200–800 kHz.

Kewalramani et al. [39], used a 10 L capacity intermediate-scale reactor operating at 700 and 950 kHz for the sonolytic destruction of Per and Polyfluoroalkyl substance (PFAS). It was demonstrated that the sonochemical efficiency of the reactor was alike to that of bench reactor (2 L) indicating the scalability of the sonochemical reactor. Moreover, for constant power density and different reactor volumes the power density showed less contribution on the sonochemistry activity, however, the sonochemistry activity was affected by lower reactor volumes for constant power of density.

The reactor geometric conditions were studied by Lee et al. [40], using an overhead stirrer and high-speed homogenizer in 28 kHz sonoreactors. It was obtained a reduction in the sonochemical activity with the extension of the height of the liquid from 2λ to 4λ and can be attributed to the geometry of the sonoreactor. Different inertial diameters and volumes (12, 17, 18, 22 and 27 cm and 2.5, 4.9, 5.4, 8.1 and 12.5 L) were used in cylindrical reactors to evaluate the sonochemical oxidation activity (Fig. 5). It was noted a reduction in the activity of oxidation as the ratio size to volume increased. The optimum size of reactor was found to be the smaller reactor with 12 cm of inertial diameter achieving around 1.7 μmol of generated I_3^- ions without the application of the mixing.

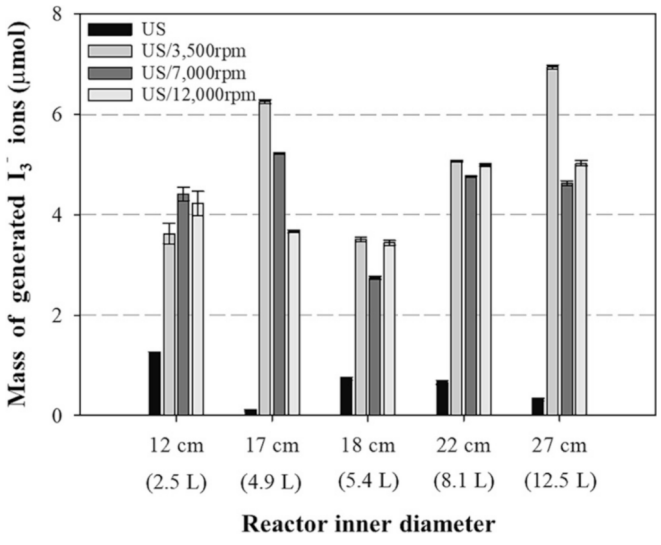

Fig. 5. Sonochemical oxidation activity (mass of I_3^- ions) using high-speed homogenizer for various reactor size contributions with liquid height of 4λ [40].

3.2.1.1. Ultrasonic bath as a source of soundwaves. The ultrasonic bath is, usually, a stainless-steel container and transducers can be installed at the bottom of the tank or at the side [63]. Based on the capacity of the tank that can be varied, more than one transducer can be introduced in the system controlling the desired frequency and power for a specific application and aiming for a more uniform acoustic field. Depending on the necessary cavitational activity, the sample can be exposed to irradiation either directly or indirectly by emerging either the sample in the bath or the reactor containing the sample in the bath using a coupling fluid respectively [5]. Most of the times the solution is indirectly irradiated, thus is of great importance to consider the position of the reactor in the system. The active zone though, is confined to a vertical plane directly above the transducers and thus to improve energy distribution, the irradiating surface area should be increased to the greatest extent feasible [64]. Even though, ultrasonic baths are conventionally used in batch mode, they can also operate in continuous mode.

In conventional ultrasonic baths, the transducer is placed in an external enclosure of the tank, not visible from outside. Other ultrasonic bath systems have an immersed transducer in the medium as was discussed in section 3.1.2.2. Moreover, the transducers can be fixed at the surface of a tube, thus becoming the soundwaves source. Then, the liquid passes through the vibrating walls of the tube for sonication [65].

A study by Rodrigues et al. [41], assessed the bioactive components' extraction from jaboticaba peels using ultrasound assisted extraction. Response resurface approach was used to evaluate how to concentration of the solvent, pH, and length of the extraction process affects the target chemical compounds (phenolics and anthocyanins). The extraction process was conducted in glass tubes placed in an open rectangular ultrasonic cleaner with internal dimensions of 14 × 24 × 9 cm and available capacity of 2.7 L. The optimal operating condition for extracting the target chemicals was for a sonication time of 10 min in a solution containing 46 % (v/v) ethanol:water, yielding 4.8 mg/g of monomeric anthocyanin and 7.8 mg/g ellagic acid (phenol).

The influence of the liquid height on sonochemical oxidation reactions was studied by Son et al. [42], employing two different bath-type sonoreactor sizes at 291 and 448 kHz, under similar electric power inputs. For 291 and 448 kHz, the largest cavitational yields were measured at liquid heights of 26 and 17 mm respectively. Furthermore, it was discovered that the liquid height at which the maximum calorimetric power was obtained, closely corresponded to the ideal liquid height for the maximum cavitational yields. Remarkably, the sonochemically active zone was not significantly inhibited by the boundaries (reactor walls), therefore there were no significant variations between the two sonoreactors. The results of this study among previously reported studies, give brief recommendations for the geometric optimisation of bath-type high-frequency sonoreactors.

$AgIO_4$ nanorods were hybridised with CeO_2 nanoparticles to create an auspicious S-scheme heterojunction. The innovative $AgIO_4$ heterojunctions were developed by Alsalme et al. [43], using a combined sol–gel and sonochemical process. More specifically, the sol mixture was immersed in a 200 W ultrasonic bath in order to homogenise the solid

matrix and promote the $AgIO_4$ and CeO_2 nanoparticles' chemical interactions. Single phase $AgIO_4$ and CeO_2 and $AgIO_4/CeO_2$ were used for Rhodamine B (RhB) degradation. Results showed that on the surface of 15 wt% $AgIO_4/CeO_2$ RhB degrades at a tenfold higher than of $AgIO_4$ and CeO_2 alone.

3.2.1.2. Ultrasonic horn as a source of soundwaves. Ultrasonic probes are commonly used in sonoreactors. In order for a sonotrode system to work effectively, it is important for the working liquid to be confined within the longitudinal high-intensity region or where the vigorous stirring takes place since there is no fluid flow. However, if big amounts of energy are applied in a high-density field which is usually what occurs at the tip of the sonotrode lots of bubbles are formed, hindering the further transmission of soundwaves, and reducing the efficiency. Likewise, continuous use of an ultrasonic probe may cause the sonicating surface to become pitted, lowering the amplitude that would have been obtained [66]. Moreover, the horn and the replaceable tip suffer from corrosion since both are immersed in the fluid. Thus, they have poor scaling prospects due to their ineffective transmission of acoustic energy into large volumes. As a result, ultrasonic probes batch systems are recommended mainly for lab-scale [64].

$Cu_2O@TiO_2$ heterojunction nanocomposites were synthesised by Kaviyarasan et al. [44], via ultrasonication aiming to employ visible light photocatalysts. The ultrasonication procedure was conducted in a 0.1 L beaker, utilising an ultrasonic horn with a probe of 13 mm diameter. Methyl Orange (MO) was used as a model contaminant to assess the photocatalytic degradation ability of the heterojunction. When doped with Cu_2O, TiO_2 maintained the structural integrity, indicating no notable morphological alterations had occurred. When exposed to light, the photocurrent of $Cu_2O@TiO_2$ was higher than that of Cu_2O nanocubes and pristine TiO_2.

A work by Mohod et al. [45], examined the ammonium sulphate crystallisation process using both the traditional and the sono-assisted approach. All experiments were performed in a 0.15 L glass beaker. Experimental parameters such as initial concentration, pH and horn depth on the width of metastable zone and average crystal size were investigated. To further understand the impact of irradiation type, ultrasound assisted crystallisation was studied using both an ultrasonic bath (50 kHz, 80 W) and an ultrasonic horn (36 kHz, 120 W). Additional stirring was not needed in the ultrasonic horn since the horn's liquid streaming was sufficient to guarantee adequate mixing. A direct mode of irradiation can be achieved by immersing the 2 cm-diameter horn tip straight into the solution while for the ultrasonic bath, an indirect way of irradiation was provided by the glass reactor suspended in the coupling fluid. Overall, the work demonstrated that, as compared to traditional cooling crystallisation, ultrasound assisted crystallisation produced better results with lower metastable zones widths, less agglomeration and improved crystal properties.

Using esterification and transesterification reaction as a two-step process and comparing the traditional method with ultrasonic systems, the sustainable generation of biodiesel from mahua oil was investigated by Gandhi and Gogate [46]. All modes of operation employed the same glass reactor with the only modification being the replacement of the water bath with the ultrasonic bath in the ultrasonic bath method. According to the required approach the stirrer or the probe was inserted through the hole at the centre of head of the reactor. The yields obtained with the conventional approach under optimal conditions were 39 %, whereas the yield attained with the ultrasonic bath and horn were 55 and 93 % respectively. When sonication techniques were compared to the standard approach, it became clear how important ultrasound is in improving mass transfer through intensive mixing and providing larger surface areas for the reaction, which in turn led to better yields of biodiesel.

A study by Son et al. [32], used a 0.5 L vessel with a 20 kHz probe sonicator that emits irradiation downward that was chosen based on both geometric and operational parameters. These parameters included the depth of the probe's immersion (vertical position), probe's horizontal position input power, liquid's height from the bottom and the bottom plate's thickness. The vertical boundaries had a positive effect on the sonochemical activity. When the probe was positioned near the vessel's bottom (60 mm of immersion depth), the liquid height at its ideal level (70 mm) and the input power was at 75 %, the probe exhibited the best sonochemical activity. According to a sonochemiluminescence analysis, when the experimental conditions were optimised, the cavitational zone progressively grew around the probe, which in turn led to an increase in the sonochemical activity. Conversely, when the probe was positioned close to the vessel's side wall, the horizontal boundaries had an adverse effect on both cavitational zone and sonochemical activity.

Rashwan et al. [47], used an immersed-type ultrasonic flat transducer probe in sonoreactor model to investigate the water sonication, using COMSOL Multiphysics. The stable acoustic pressure zone was not affected by varying the depth of the transducer probe from 20 to 100 mm. Also, the maximum pressure remained persistence while the minimum was rather fluctuated with the increase of immersion depth, whereas the acoustic waves reflected off from the bottom walls of sonoreactor, the reflected wave interfered with the incident wave leading to either construction or deconstruction wave interference. In addition, up 10 times the sonoreactor was scaled with the acoustic power source. It was observed that the greatest amplitude of acoustic pressure was 5.85 $x10^5$ Pa for the lab-scaled sonoreactor while for the up-scaled reactor the acoustic pressure was lower by 24.6 % and indicated that the cavitation area was minimal and cannot sustain the bubble effectively.

3.2.1.3. Ultrasonic Cup-Horn as a source of soundwaves. Sonochemical cup-horn is another component used in batch reactors, combining the advantages of the sonotrode and bath reactors. The cup-horn is installed inside the vessel, as seen in Fig. 6, allowing a more homogeneous ultrasonic distribution and the sonication of more than one samples simultaneously with equal transmission of soundwaves [67]. They are able to transmit 50-fold higher energy than bath systems and tend to be less corrosive than ultrasonic horn-batch systems enabling highly acidic liquids in the system. Ultrasonic cup-horns are preferred usually for indirect sonication, also lowering the risk of contamination [12].

A study by Bizzi et al. [48], studied the conversion of lignocellulosic materials into furfural by using ultrasonic energy. Several lignocellulosic materials were subjected to the ultrasound-assisted acid hydrolysis (UAAH) method and parameters such as reaction duration, ultrasonic amplitude, and feedstock amount were evaluated. The mixture was inside of a glass reactor and was subjected to soundwaves using an ultrasonic cup-horn system (76 mm diameter, 165 mm long) operating at 20 kHz, 30 °C and 50 % amplitude. At 60 min of sonication, the produced furfural yields were 72.4 ± 4.3 mg/g. The impact of ultrasound for furfural synthesis was demonstrated by comparing the findings to those attained at silent settings (mechanical stirring) under identical reaction conditions.

Santos et al. [49], studied the ultrasonic energy application for the UAAH of cellulose to create chemical blokes. Three different ultrasonic systems (bath, probe and cup horn) were used to study the conversion of microcrystalline cellulose, testing a number of acid mixtures in a glass cylindrical reactor. A 20 kHz, 750 W ultrasonic processor was used connected to either the titanium probe (13 mm diameter, 254 mm long) or to the cup horn (76 mm diameter, 165 mm long). The experiments conducted in ultrasonic baths were running at 25, 35, or 37 kHz with power of 100, 200, or 330 W respectively. Following process optimisation, 78 % conversion to furfural was achieved with a 4 M HNO_3 solution that was sonicated at 30 °C, 50 % amplitude for 60 min in a cup-horn system. The authors concluded that the utilisation of a diluted acid solution in conjunction with this moderate temperature marks a

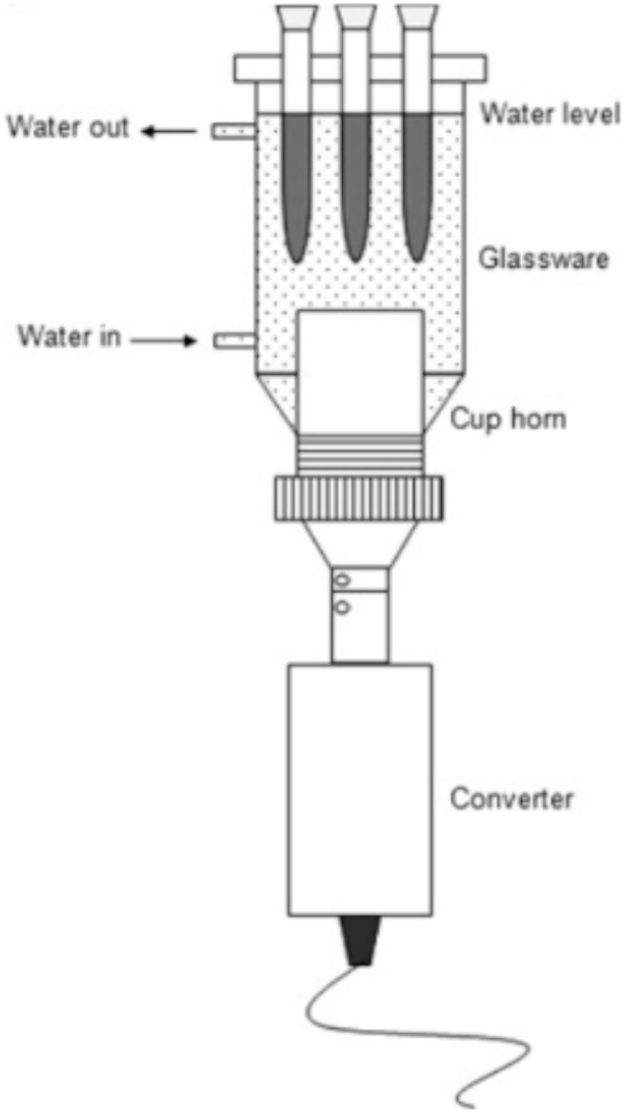

Fig. 6. A schematic illustration of an ultrasonic cup-horn batch system [67].

significant advancement in the selective synthesis of chemical building blocks via ultrasonic radiation.

Ultrasound-assisted hydrothermal process was used by Zargazi and Entezari [50] to synthesise Bi_2WO_6 nanostructures. A glass beaker was immersed in a cup-horn (20 kHz, 750 W, 40 % acoustic amplitude) for an indirect high intensity sonication. Hydrothermally synthesised Bi_2WO_6 nanostructures were also examined to evaluate the impact of ultrasonic waves on the morphology. The sonosynthesised sample's higher crystallinity than the conventional sample was verified by XRD. Moreover, the results demonstrated that ultrasound reduced the particle size and the flower-like structures created by sonication include many hollow spots compared to the hydrothermal sample increasing the dispersion of visible light. The synthesised nanostructures were tested for the photocatalytic, sonocatalytic and sonophotocatalytic degradation of RhB/MB as a pollutant, where the sonophotocatalytic process exhibited the best results from the sono-synthesised sample.

3.2.2. *Ultrasonic continuous flow reactors*

Continuous flow reactors are also available for sonochemical reactions. They are becoming more popular since they achieve higher production rates and enhanced yield due to their shorter reaction times, when compared to batch systems, and they can be scaled-up for industrial applications. However, a lack of understanding regarding the design, the functionality and their performance characteristics limit their application. For the batch systems, the liquid/vessel ratio played a significant role in the reactor design as it was discussed above. Even though this is also important for the continuous flow systems, another important aspect is the amount and position of transducers in order for the solution to be fully sonicated as it passes through the reactor.

Metastable cadmium sulphide (CdS) nanoplatelets were developed by Palanisamy et al. [51], using a continuous flow sonochemical reactor. The flow cell was designed taking into consideration the ultrasound attenuation as a function of distance in front of the ultrasonic horn. Reducing the residence time inside the reactor is also a crucial point of the flow cell's design. Thus, an insert was employed to alter the flow cell's internal volume, decreasing the volume from 65 to 8 mL, resulting in shortening the fluid residence time in the reactor. The clearance between the insert's inner diameter and the horn's outer diameter was big enough to avoid vapour lock and still be greater than the crucial bubble size. Moreover, it was found that the insert improved the flow cell's internal temperature uniformity. The results of the synthesis were compared to those from batch systems that employed ultrasound-induced heating or conventional heating. It was discovered that hexagonal platelets of CdS with cubic crystal structures with thickness far below 10 nm were produced by continuous sonochemical synthesis. When compared to batch synthesis methods, the continuous sonochemical process yields substantially higher particle size homogeneity and product throughput.

The sonochemical and mechanical impacts on aluminium erosion were evaluated using KI oxidation on a continuous ultrasonic system and a batchwise system employing the same transducer technology by Eric Loranger et al. [52]. For the batch system a direct application of ultrasound and an indirect using a glass reactor were studied using 12 transducers connected in two groups of six. The ultrasonic flow-through reactor was a more complicated system, consisted of a mixing tank, a pump and different piping. The ultrasonic tube of the ultrasonic flow-through reactor jacket had 24 transducers, connected in four groups of six. The findings showed that the glass reactor had a notable effect on the sonochemical's effect attenuation, especially at higher frequencies (170 kHz), where less I_3^- radicals were produced. In contrast, the sonochemical effects at 170 kHz in the flow-through sonoreactor were 79 % greater than those at 68 kHz. Irradiating 11.2 s per minute of operation, the continuous sonoreactor demonstrated a 33 % greater sonochemical effect over the ultrasonic bath.

The treatment of common petroleum products using the ultrasonic-assisted oxidative desulfurization (UAOD) technology was the focus of a research project conducted by Shamseddini et al. [53]. A pilot flow-through sonoreactor was designed and built based on the optimum conditions from a prior batch experimentation to determine the impact of operating parameters on sulphur removal efficiency. Along the reactor's bottom side, two transducers with a frequency of 20 kHz were installed so that the incoming flow was fully developed exactly before reaching the first transducer. The removal efficiency in the batch phase, which was 61 %, might reach nearly 80 % in the continuous reactor and with increasing the power, the sulphur removal efficiency is higher. Potential effects of ultrasonication on kinematic viscosity and boiling point distribution on the cracking of gas oil samples were also investigated. Notably, UAOD's impact on the kinematic viscosity of commercial gas oil is unpredictable, and the removal of sulphur doesn't guarantee viscosity reduction. Additionally, while pure sonication decreases viscosity, the effect is dependent on ultrasound power.

3.2.2.1. Multiple frequency emitting walls. Continuous flow cells are a suitable option for large scale sonochemical reactors [68]. In more detail, the flow cell has transducers attached to the reactor wall. By utilising many transducers, it is possible to get more consistent cavitational activity by adjusting the pitch of the numerous transducers [69]. When utilising multiple frequencies at the same power dissipation, it is

possible to achieve both chemical and physical effects, as well as strong cavitation, in comparison to using only one frequency. Additionally, the decoupling losses can be decreased as a result of the lower power dissipation per transducer, increasing the amount of energy available for the intended transformations. The ability to concentrate intensity at the core zone away from the transducers is another benefit of the multiple transducer unit design, which reduces surface erosion and localised cavitational activity [5].

The flow cell's size and length can be altered depending on the processing conditions and treatment durations. Rectangular and hexagonal geometries can be employed (Fig. 7). It is noteworthy to add that in comparison to hexagonal flow reactors, cylindrical geometry inflow reactors are more highly suggested since they offer a better reflection of the ultrasonic field. A cooling system can be added to regulate the medium's temperature [70]. It is also possible to alter the flow cell design to incorporate an annual quartz tube, UV-lamp equipped, in the centre of the reactor that can enable simultaneous energy dissipations based on the application of UV and ultrasonic radiations.

The effectiveness of a novel ultrasonic flatbed reactor for the pretreatment of three distinct waste activated sludges was examined by Lippert et al. [54]. The impact of a certain energy input on the degree of disintegration (DD_{COD}) and increase of methane generation was methodically examined in this study. As shown in Fig. 8, the lab-scale reactor (100 × 8 × 4 cm) had six externally placed ultrasonic transducers (3 transducers each) at the top and bottom walls of the chamber. The system was running at a 25 kHz frequency and 300 W power. Ultrasonication has demonstrated a considerable increase in methane yields even at low energy inputs and DD_{COD} levels.

Another study by Lippert et al. [55], investigated the flow of water in an ultrasonic flatbed reactor containing two sewage sludge substitutes (transparent xanthan solutions that resemble waste activated sludge −WAS and digested sludge-DS with identical flow behaviour). The reactor set-up is similar to the previous study with dimensions of 100 × 8 × 8 cm. By injecting into the bulk liquid the dye streams, the flow was made visible. When ultrasonication was used on water, the liquid was completely mixed, but the dye streams in sewage sludge were mostly in laminal flow and were only mildly distributed. The authors concluded that in ultrasonic flatbed reactors, cavitation-induced microturbulence does not significantly mix the viscous materials but further study should confirm these findings.

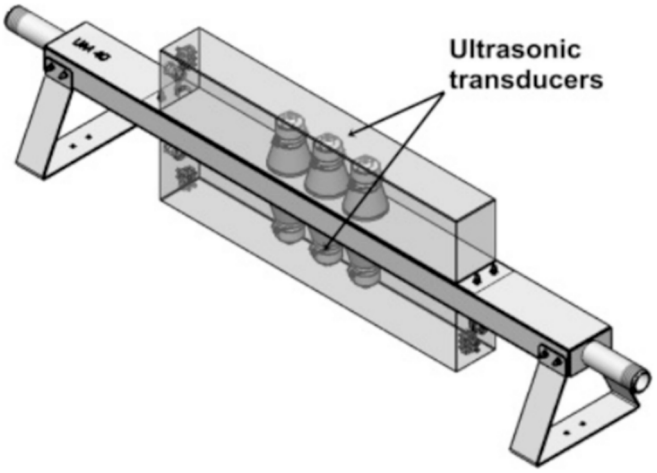

Fig. 8. Schematic representation of the ultrasonic flatbed reactor [54].

Two new pilot-scale reactor designs were tested from Kumar et al. [56], for the cavitational activity distribution. A longitudinally vibrating horn was utilised in the first experiment, placed in 7.5 cm above the bottom of the reactor. Hexagonal flow cell was used in the second experimental set-up. Three circular transducers were installed on each side of the flow cell with 3 cm of distance between each transducer. Results showed that in both cases, a nearly uniform distribution of the cavitational activity is achieved. In contrast to a traditional immersion type horn, with a cavitational activity variation by nearly 80–400 % over a very small distance in both axial and radial directions, the cavitational activity variation has been found to be in the range of 10–30 %. This work demonstrated that each of the two designs could function well in large-scale operations with the hexagonal flow cell design being a better option for scale-up.

3.2.2.2. Microflow reactors. Micro-structured reactors are also being used for continuous processes due to their more effective setup than batch reactors [71]. Their benefits include excellent mass and heat transfer, a large specific surface area, safety, energy efficiency and finer process control. Despite these advantages, channel clogging is a significant drawback that restricts the usage of microreactors in flow that contain solid particles or where solid particles are expected to form. The fact that bubbles of a size of comparable to the channel walls may find it difficult to collapse by cavitation is another restriction on the use of the microreactor in conjunction with the ultrasound. Fig. 9 shows a set-up of a microflow sonoreactor for nanoparticles synthesis. Microreactors can

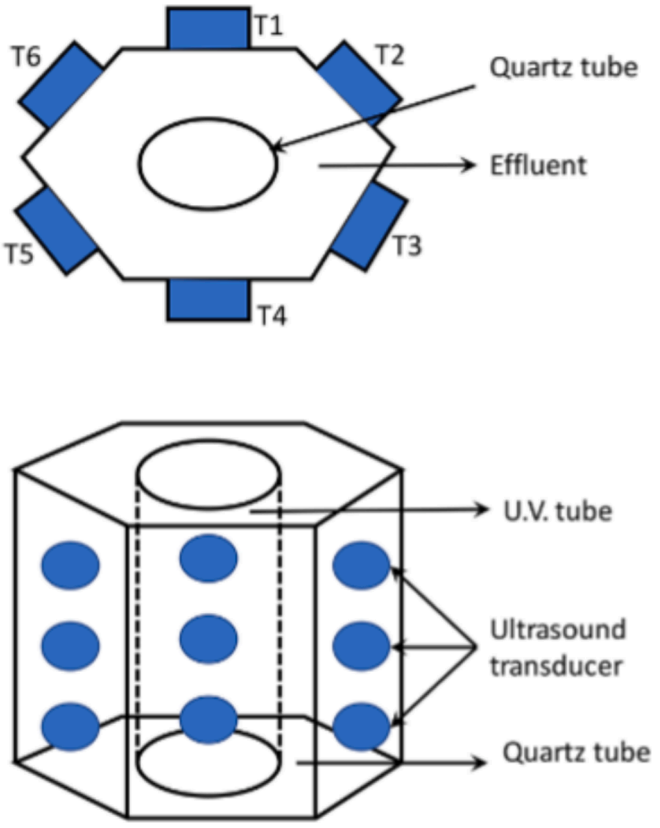

Fig. 7. Schematic illustration of a hexagonal flow cell with six transducers [70].

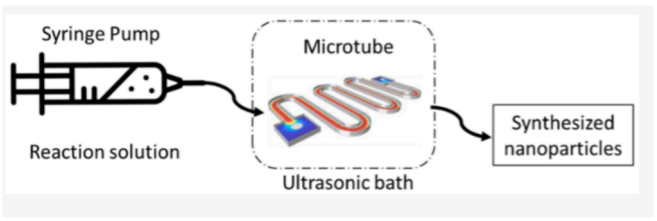

Fig. 9. Concept of microflow ultrasonic reactor for the synthesis of nanoparticles [71].

be scaled up to enhance production by expanding their characteristic dimensions, however doing so will also cause the intensification advantage to be lost. Scaling out microfluidic devices can effectively circumvent the drawback to some extent. Scaling out simply means adding more microreactors to create parallel network, as opposed to increasing the size of the microreactors [72].

A work by Colmenares et al. [57], presents a novel approach that uses ultrasound technology to deposit TiO_2 nanoparticles on the inner walls of a hexafluoropropylene tetrafluoroethylene (FEP) microtube. An ultrasonic 3 mm micro-tip probe was placed in the sonoreactor and 5 cm of the FEP microtube were exposed to ultrasound. Surface alterations were spotted during the sono-assisted process such as etched and rough areas. With the use of a syringe pump, the TiO_2 homogeneous suspension, was forced through the FEP microtube. Under ultrasound, the capillary pulsed the suspension at a rate of 0.025 mL/min for 30 min. The alterations observed above made it easier for TiO_2 nanoparticles to be stabilised on the internal walls of the FEP microtube. The TiO_2-U-FEP microtube's photocatalytic activity was tested with phenol photocatalytic degradation in water, giving higher efficiency (TOF = 0.41 1/s) than that which had been previously reported in a traditional batch photoreactor using UV light (TOF = 0.03 1/s).

A Methyl Orange (MO)-containing aqueous solution was sonicated in a polydimehylsoloxane/glass (PDMS/glass) microreactor by Thangavadivel et al. [58]. A water bath contained the transducer and microreactor which was made up of four channels with 100 mm height. During operation, the bottom of the reactor plate was placed 8 mm above the transducer functioning at 200 kHz and to guarantee optimal energy transfer to the microreactor, the centre lines of the transducer and the reactor were vertically aligned. At 20 °C and pH 2, 5 mg/L MO solution was circulated at a flow rate 0.76 mL/min, resulting in removal efficiency of 9 %. Increasing the acoustic power, MO concentration and flow rate the removal efficiency also increased but an increase in temperature was associated with a lower removal efficiency. Additionally, under the same experimental conditions, a 4 % rise was seen upon adding 100 mg/L of CCl_4.

Ultrasonic batch systems, characterised by low cost and enhanced mixing, suffer from non-uniform acoustic fields, challenging control, and scalability. Ultrasonic baths provide versatility, accommodating various capacities and operating modes; however, their active zone is confined, demanding efforts to improve energy distribution. Ultrasonic probes, though common, are limited to lab-scale due to potential scaling issues, corrosion, and reduced efficiency. Sonochemical cup-horns offer homogeneous ultrasonic distribution and simultaneous sonication of multiple samples while transmitting higher energy. Continuous flow reactors boast higher production rates, yet limited understanding of design hinders commercial use. Multiple frequency emitting walls offer consistent cavitational activity even in large-scale reactors, reduce surface erosion and decoupling losses. Microflow reactors have excellent mass and heat transfer, but face challenges like channel clogging and potential scaling issues. The choice between systems should align with desired outcomes and the nature of the process involved.

4. Effect of operating parameters

A number of parameters including the temperature, the intensity of irradiation, the frequency of ultrasound, the pressure of amplitude, the sonication time and the geometry of the reactor need to be optimised to successfully carry a reaction in a sonochemical reactor. In this section, different parameters were analysed in order to understand better their effect on the ultrasound cavitation and activity. The frequency of ultrasound, pressure amplitude and the reactor design are regarded as 'primary' parameters as these fundamental parameters constitute the base that needs to be considered for the working set-up of a sonochemical system [73]. Table 2 summarises the findings of the studies discussed below at different sonochemistry operating parameters.

Table 2
Sonochemistry operating parameters.

Parameter	Substance	Efficiency	Ref.
Frequency of ultrasound	Ampicillin (AMP)	59 % removal at 375 kHz and 30 min	[74]
Frequency of ultrasound	Rhodamine B (RhB)	81 % degradation at 576 kHz	[75]
Frequency of ultrasound	H_2O/O_2	5.6 x10^{-19} mol H_2 at 200 kHz	[76]
Temperature	Toluidine blue (TB)	53 % removal at 50 °C and after 30 min	[77]
Temperature	Rutin	20 % degradation at 10 °C	[78]
Temperature	cy-3-gly	34.5 % degradation at 10 °C	[78]
Intensity of irradiation	Ammonia	69 mg N (g VSS)$^{-1}$ d^{-1} specific Annamox activity at 1.1 W cm^{-2}	[79]
Intensity of irradiation	*T. lanuginosus* (TL) lipase	39 % enhanced activity of TL lipase at 11.37 W cm^{-2}	[80]
Intensity of irradiation	CALB lipase	62 % enhanced activity of CALB lipase at 15.48 W cm^{-2}	[80]
Sonication time	Food waste	18500 mg L^{-1} sCOD at 10 min and 0.4 W mL^{-1}	[81]
Sonication time	GNP@MWCNT	40.6 mV zeta potential at 120 min	[82]

4.1. Frequency of ultrasound

The ultrasound frequency is amid the most major parameters that the sonochemical reactions and intensity by acoustic cavitation are depended, as the number of produced cavitation bubbles increase with the frequency [1]. Montoya-Rodríguez et al. [74], performed in the first place, the sonochemical elimination of ampicillin (AMP) antibiotic using two operation modes (pulsed and continuous) in a Meinhardt ultrasound reactor. The degradation performance of AMP was evaluated at 375 and 990 kHz, with the first one achieving the best antibiotic removal (up to 59 %) in 30 min of treatment as well as highest H_2O_2 concentration that was accumulated (Fig. 10). At 375 kHz frequency, due to the higher H_2O_2accumulation, the production of hydroxyl radical is also higher where the results are attributed.

The ultrasonic frequency effect at lower and higher frequencies was investigated by Bößl et al. [75]. More sizeable reactors with volumes of 500 and 1000 mL were used in their investigation, in comparison to other studies with smaller sonoreactors up to 100 mL volume. Rhodamine B (RhB) aqueous solution was used to perform the study in an extensive scale of frequencies, from 20 kHz to 1 MHz. Phenomena such as sonochemistry and sonocatalysis often occur during the investigation of piezocatalysis and an acoustic field is generated by ultrasound. FEM simulations were occurred at 20, 35, 576, 864 and 1142 kHz, and it was expected that at 864 kHz, which is a global resonance frequency, to achieve the best piezocatalytic effect as the 'top-to-bottom' electric

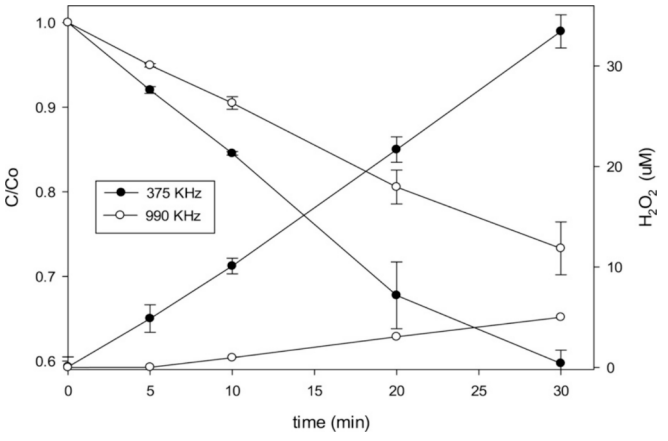

Fig. 10. Ultrasonic frequency effect on the AMP degradation (C/C_0) and H_2O_2 accumulation [74].

potential difference of 69.1 V was the greatest. However, the experiments of RhB degradation showed a completely different results compared with the simulations. At low frequencies, the experimental results without the presence of piezocatalyst, showed low dye degradation, around 11 and 29 % at 20 kHz and with the addition of piezocatalyst, between 14 and 35 % at 32–38 kHz. The degradation of RhB at higher frequencies was found to be high with the most significant degradation (81 %) to be obtained at 576 kHz and the addition of piezocatalyst didn't show any significant difference in the results.

Asakura and Yasuda [83], examined the frequency effect on the ultrasonic degassing for degassed water and air-saturated water in a double-cylinder structured vessel. The evaluation of ultrasonic degassing occurred by the dissolved oxygen concentration in the water. A 100 mL water sample was used at frequencies 22, 43, 129, 209, 305, 400, 1018 and 1960 kHz and 101.3 kPa pressure. It was shown that the ultrasonic degassing rate was higher between 200 kHz and 1 MHz whereas the bubbles grew because of the ultrasonic irradiation, the dissolved gas in the water moved into the bubble as gas and the dissolved gas in the water was decreased. However, ultrasonic degassing and sonochemical efficiency hinge on the cavitation bubbles number as degassing and chemical reactions occur by cavitation and assume that the dependance of ultrasonic degassing on frequency is similar to that of sonochemical efficiency.

The ultrasound frequency is a parameter that affects the number and the size of bubbles, the cavitation threshold and the collapse temperature. Hence, the rise of sonochemistry frequency decreases the bubble size and also the bubbles collapse fast without achieving the maximum size. It is also suggested that an upper limit of the applied ultrasound frequency exists, while at lower frequencies the cavitating bubbles can grow for longer period as the time length of the acoustic cycle is longer and their collapse results more mechanical effects [75].

4.2. Temperature

Chadi et al. [77], assessed the temperature effect of the liquid on the degradation of toluidine blue (TB) in a cylindrical water-jacketed glass sonoreactor. The experiments occurred between 25 and 70 °C under 15 W and 1700 kHz for two different initial concentration of TB, 0.5 and 10 mg L^{-1}. It was found that the rise of temperature of the liquid from 25 to 60 °C did not affected the degradation kinetics at TB initial concentration of 0.5 mg L^{-1} while at 70 °C a reduction in the degradation performance was observed. For the highest concentration of TB, 10 mg L^{-1}, an improvement was observed with the temperature from 25 to 50 °C and the additional increase of temperature up to 70 °C demonstrated that the degradation rate declined. At the optimum temperature of 50 °C, the efficiency of removal was found to be 53 % after 30 min.

The evaluation of the impact of sonochemical effects and mechanical effects on the polyphenols reduction was occurred by Wang et al. [78]. Three different polyphenols, caffeic acid, rutin and cy-3-glu were utilised to study the temperature effect on their extraction yield. Temperatures between 10 and 70 °C were investigated with the polyphenols rutin and cy-3-gly to have the favorable degradation rate at the lowest temperature of 10 °C (20.23 % and 34.41 %) due to the boost of sonochemical effects at low temperatures. It was concluded that the two polyphenols were more likely to go through the free radical degradation rather than the thermal degradation. Moreover, inside the bubble, the peak pressure is responsible for the mechanical effects while the peak temperature is controlling the sonochemical effects. For the extraction of polyphenols, their tolerances to heat and free radicals must be taken into account because of the efforts of free radical degradation under low temperature or thermal degradation under high temperature.

Another study occurred by Lin et al. [84], examined the effect of sulfate ions on the degradation of perfluorooctanoic acid (PFOA) by ultrasonic irradiation at various temperatures. The PFOA decomposition took place at temperatures of 25, 35 and 45 °C with and without the presence of sulfate ions and the results revealed that the maximum rates of decomposition and defluorination efficiencies were obtained at 25 °C. Moreover, it was assumed that the temperature increase inhibited the direct and indirect mechanisms which might be due to the lower surface tension at higher temperatures.

4.3. Intensity of irradiation

The ultrasonic irradiation producing cavitation generates transient bubbles and their implosion generates different chemical and physical phenomena and demonstrate a remarkable role in the synthesis of nanostructured materials [85]. The irradiation intensity is explicated as the power dissipation per unit area of transducers used in irradiation.

Anaerobic ammonia oxidation (Anammox) reaction took place in a lab-scale ultrasound assisted Anammox reactor (ABR) to find the optimal ultrasound parameters by Yuan et al. [79]. The investigation of the exposure time and ultrasound intensity effect on specific Anammox activity (SAA), batch tests occurred. Different ultrasonic intensities of 0.3, 0.5, 0.8, 1.1, 1.4 and 1.6 W cm^{-2} were used with the ultrasonic intensity of 1.1 W cm^{-2} to exhibit the best SAA with a value of 69 mg N (g VSS)$^{-1}$ d^{-1} at 40 sec of exposure time (Fig. 11).

Nadar and Rathod [80], investigated how the ultrasonic intensity affects the activity of TL lipase and CALB lipase. It was derived that the maximum enzyme activity was achieved at ultrasonic intensities of 11.37 and 15.48 W cm^{-2}, for TL lipase and CALB lipase, respectively. Additional rise in the ultrasonic intensity caused the gradually minimisation of the activity of lipases, as the high intensity ultrasound might improved the cavitation effects and could have damaged the polypeptide chains and led to the inactivation of enzymes. Stable cavitation is obtained at mild-intensities and low-frequencies ultrasound irradiations.

4.4. Pressure amplitude

The pressure amplitude is considered one of the primary parameters for the sonochemical reactor design. This parameter is related with the conveyed power to the liquid and can escalate the cavitation bubbles number, the temperature of collapse and the sonochemical yield. The pressure amplitude has upper and lower limits and being above the upper limit coalescence and degassing occurs with limited active cavitation while being below the lower limit the amplitude of the sound field is very small to cause bubble growth. The increase of pressure amplitude increases the number of cavities available which will face structural instability because of the increase of the collapse force [73].

Yamamoto et al. [86], investigated the fragmentation mechanism and dynamic behavior of cavitation bubbles under small pressure amplitudes of ultrasound waves through 3D simulations and experimental observations. It was observed through experimental and simulation studies using the Keller or Rayleigh-Plesset equation, that a 20 μm bubble oscillates linearly at small pressure amplitudes and non-linearly at large pressure amplitudes. At low pressure amplitudes the oscillation of bubbles is synchronised with the surrounding pressure field and while the pressure amplitude increases the temperature at the center of the bubble oscillates drastically and during the bubble contraction or expansion an oscillation phase shift is occurred and leads to the non linear bubble oscillations.

The bubble oscillation was investigated by Yamamoto and Komarov [87], showing that at larger pressure amplitudes the bubble becomes non spherical. In addition, two bubble cycles were conducted, and the amplitude of oscillation was assessed during the second cycle at sound pressure amplitudes of 0.5, 0.7 and 0.9 atm. Under the latest pressure amplitude, the bubble shape became non spherical as the size of bubble enlarged at the beginning of the second cycle and therefore, the bubble oscillations were examined in the first cycle at pressure amplitude of 0.9 atm. It was observed that the cavitation bubble oscillation amplitude became bigger in the multi-bubble system compared to that in the single-bubble system due to the acoustic wake effect.

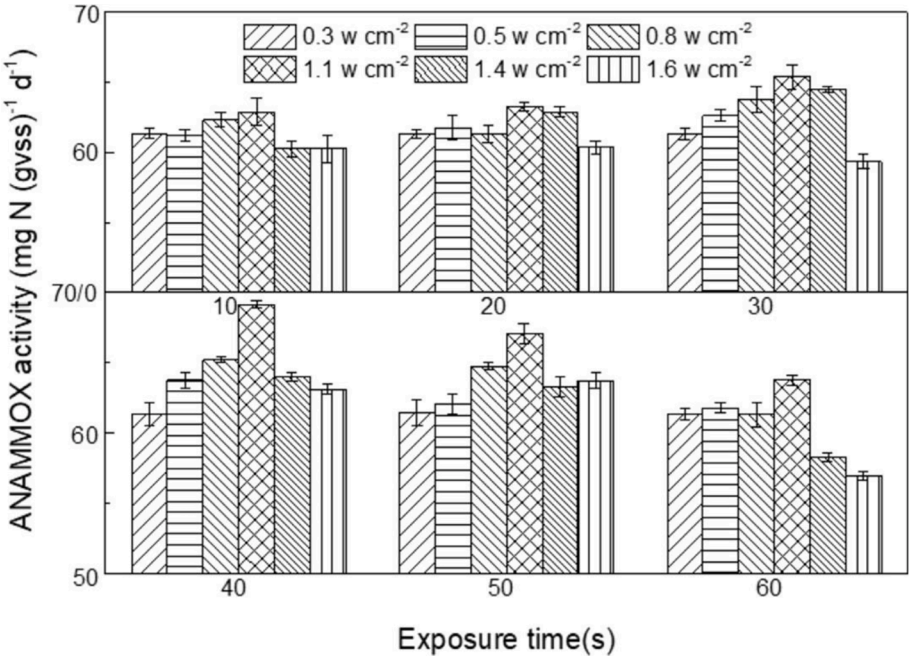

Fig. 11. The effect of different ultrasound intensities and exposure time on the Anammox activities [79].

4.5. Sonication time

Typically, the cavitation yield is increased with the operation time but beyond a certain time reduced yields can be obtained. Many studies examined the effect sonication time [88–92]. Joshi and Gogate [81], studied the ultrasound assisted food waste feedstock pretreatment to enhance the production of biogas through the anaerobic digestion process. Irradiation times from 2 to 14 min were used in order to examine the dependence of the variations in the soluble chemical oxygen demand (sCOD) on the sonication time, while the ultrasound density was constant at 0.4 W mL^{-1} (Fig. 12). It was obtained that the sCOD reached maximum in the case of 10 min with a value of 18500 mg L^{-1} which was about 1.6 times greater than that obtained in the case of 2 min. Also, an insignificant difference in the results was observed at 10 and 12 min, while the further increase of time at 14 min lead to the reduction of sCOD to 17200 mg L^{-1}. The optimum time-period of ultrasound irradiation relies upon the complication of the material and longer periods of time might show degradation of solubilized contents due to excessive cavitation.

Ghafurian et al. [82], investigated how the ultrasonication duration affects the rate of evaporation of a composite based nanofluid containing multiwalled carbon nanotubes/graphene nanoparticles (GNP@MWCNT). The samples produced had pH between 7 and 8 and grew moderately with the ultrasonic time up to 120 min. The increase of the ultrasonic time resulted the growth of a repulsive force amid the nanoparticles and to separate from each other and the dispersion of

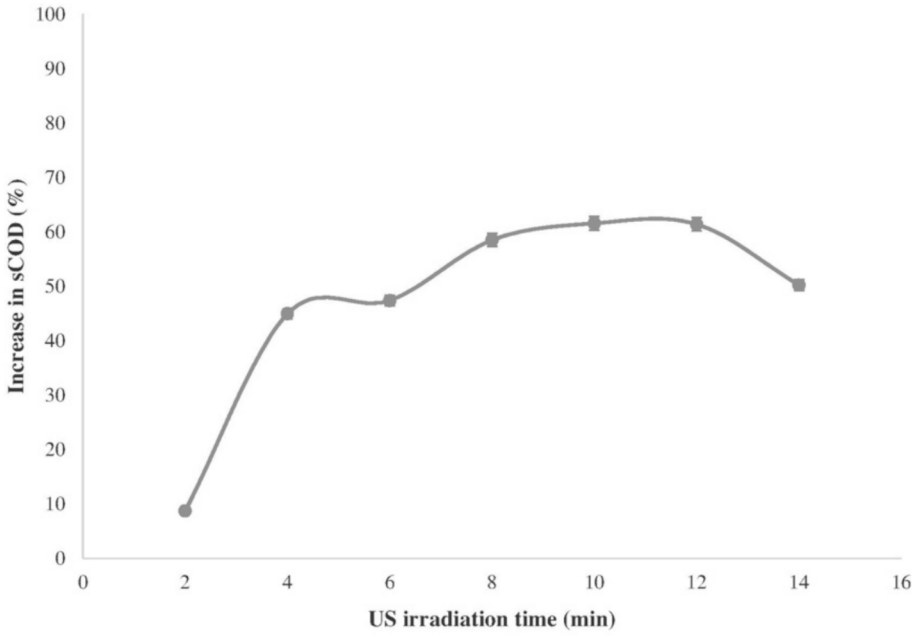

Fig. 12. Ultrasonic irradiation time effect on sCOD of food waste [81].

nanoparticles to enhance in the base fluid. Moreover, the increase of ultrasonication period from 30 to 120 min, caused the increase of zeta potential from 33 to 40.6 mV. The further increase of sonication time up to 240 min, demonstrated that the zeta potential decreased around 28.8 mV. The increase of zeta potential values and nanofluid stability could be attributed to the pH adjustment.

Concluding, the ultrasound frequency dramatise a principal role on the size and the number of the bubbles and considered one of the primary parameters. The optimum frequency results more effective collapse achieving extremely high temperatures and pressures. The temperature of the bulk is another parameter that influences the sonochemical activity. The increase of temperature often inhibits the reaction as mentioned above due to the different mechanisms occurring. Additionally, an optimum intensity of irradiation and sonication time exists. The intense collapse of the bubbles is usually obtained at lower operating intensities. As for the pressure amplitude which is another important parameter, is related with the bubbles size and the number, the temperature collapse and the yield of the reaction leading to more violent collapse.

5. Applications

5.1. Biochemical engineering

Sonochemistry has lots of applications in biochemical engineering. Acoustic and hydrodynamic cavitation can improve the effectiveness of microbial cell disruption, one of the most known applications of biotechnology (Fig. 13). Another application is microbial disinfection in water, due to its remarkable effects on the formation of hot spots, extremely reactive free radicals and turbulence linked with liquid circulation that can replace physical and chemical methods with significant disadvantages that have been used throughout the years to disinfect microorganisms in water [93].

Ethanol produced from lactose through fermentation using *Kluyveromyces marxianus* under different sonication regimens was reported by Sulaiman et al. [95]. Using 10 %, 20 %, and 40 % duty cycles, fermentations were conducted at low-intensity sonication (11.8 W/cm^2), in a stirred bioreactor with 3 L of working capacity (Fig. 14). In comparison to the control (no sonication), ethanol production increased throughout all duty cycle tests with the 20 % cycle being the optimal. Under ideal conditions, the final ethanol concentration (5.20 $\pm$ 0.68 g/L) was over 3.5 times higher compared to control. Duty cycles at 10 % and 20 % seemed to promote yeast growth but at 40 % a discernible negative effect was observed on cell growth, but the cell viability stayed over 70 %.

A study by Wang et al. [96], examined the efficacy of high-frequency focused ultrasound (HFFU) on the microalgal cells disruption. *Scenedesmus dimorphus* and *Nannochloropsis oculate*, two microalgal species, were treated with a low-frequency non-focused ultrasound (LFNFU) at 100 W and 20 kHz and focused ultrasound operating at 40 W and 3.2 MHz. The results showed that HHFU was successful in disrupting microalgal cells, as evidenced by the treatments' considerable increases in lipid fluorescence density, reductions in cell diameters, and increases in chlorophyll-a fluorescence density. The HFFU treatment used less energy than the LFNFU treatment. Moreover, it was discovered that combining low- and high-frequency treatments was more successful than using just one frequency treatment during the same processing period.

A study by Yamamoto et al. [97], examined the impact of a 20 kHz low frequency using a sonotrode and at 580, 864, and 1146 kHz using a multi-frequency bath on suspensions of *Chlamydomonas concordia* and *Dunaliella salina*. The decrease in the number of algae was affected by both frequency and acoustic power. The effect of ultrasonic disruption on *C. concordia* was found to be $20 < 585 < 864 < 1164$ kHz, while for *D. salina* was $20 < 580 \cong 864 \leq 1164$ kHz. High-frequency sonication is clearly more efficient for cell disruption in both species than traditional low-frequency sonication. In addition, the mechanical characteristics of the cell were found to be related to the appropriate disruption frequency for every type of algae.

The effectiveness of sono-disruption of Chaetoceros gracilis, Chaetoceros calcitrans, and Nannochloropsis sp. was examined by Kurokawa et al. [98], by subjecting algal suspensions to ultrasonic waves at different frequencies ranging from 0.02 to 4.3 MHz. The findings demonstrated that the amount of algae reduced was frequency dependant, and the greatest efficiency for C. gracilis, C. calcitrans, and Nannochloropsis sp. was attained at 2.2, 3.3, and 4.3 MHz respectively. Free radicals were probably not involved in the algal disruption process, but cavitation bubbles were, based on the direct and chemical effects of ultrasonication.

5.2. Petrochemical industry

One potential solution to reduce pollution from the petroleum refining process is sonochemistry. According to a number of research, ultrasonic cavitation can be used to increase the quality and upgrading of crude oil (Fig. 15). Chemical additives are used to reduce the viscosity of crude oil during the cracking process. Several recent studies demonstrated that ultrasonic waves have the potential to make additives more soluble in crude oil which eventually reduce viscosity by lowering interfacial tension. Often oil-soluble dispersive catalysts treated with acoustic cavitation are frequently employed to enhance crude oil's viscosity reduction. Most of the research assessed the impact of ultrasonic waves on the viscosity reduction of heavy oil while only few researches have been done on the structural alterations of crude oil components treated with acoustic cavitation [99].

In a study by Sawarkar et al. [100], acoustic cavitation was applied to three petroleum residues- the Arabian mix vacuum residue (AMVR), the Bombay high vacuum residue (BHVR) and Haldia asphalt (HA)- for varying response periods ranging from 15 to 120 min at room temperature and pressure. Experiments with ultrasonic bath (20 kHz, 120 W) and horn (20 kHz, 150 W) took place to compare the effectiveness of two acoustic cavitation devices, in terms of their capacity to convert petroleum residues into lighter products with higher added value. Results showed that petroleum residues can be effectively upgraded via acoustic cavitation as seen by the samples' decreased asphaltene content and increased saturates and aromatics. Ultrasonic horn was more efficient than ultrasonic bath in converting the residues into value-added

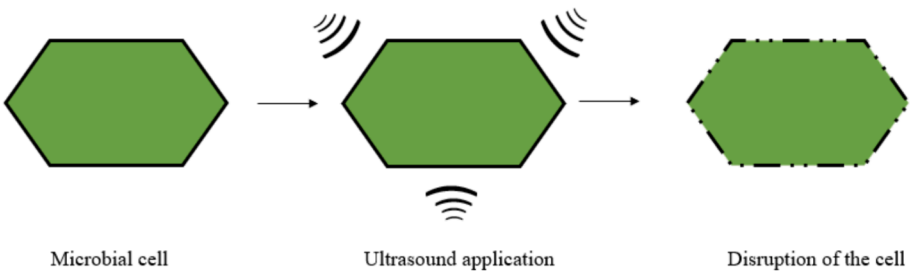

Fig. 13. Ultrasound-assisted membrane disruption of a microbial cell [94].

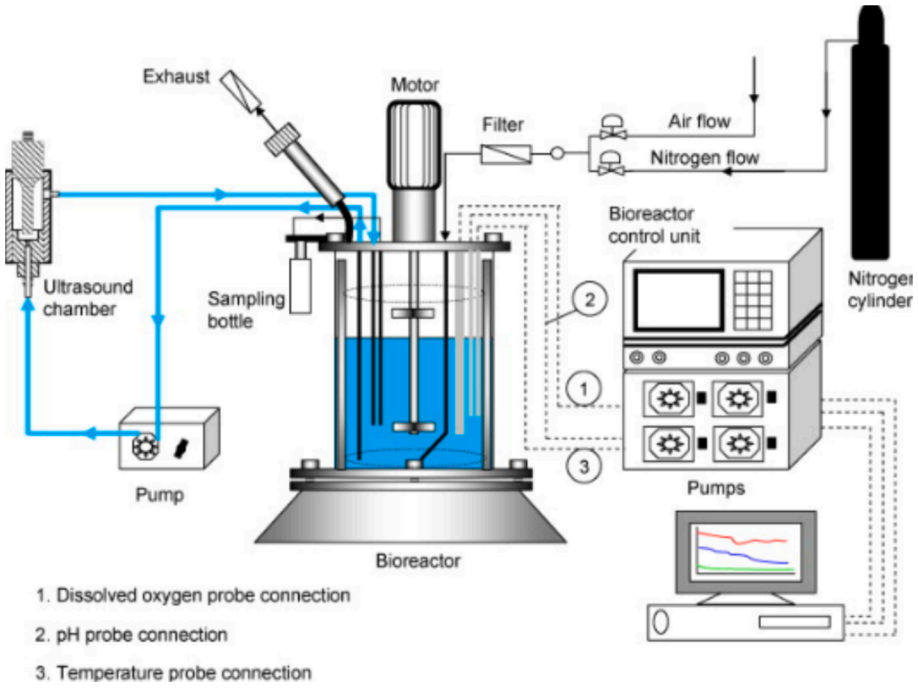

Fig. 14. Ultrasound assisted bioreactor for fermentation process [95].

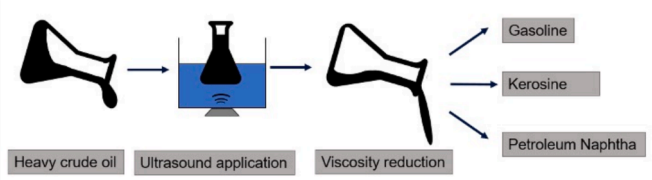

Fig. 15. Application of ultrasound in heavy crude oil sample.

products and there was about 51 %, 48 %, and 39 % greater reduction in the content of asphaltenes in AMVR, BHVR and HA, respectively.

The structural alteration of Tache heavy oil components treated with ultrasound, which was facilitated by nickel oleate were examined by Cui et al. [99]. An ultrasonic wave cell pulveriser with a 20 kHz frequency was employed. For the cavitation treatment, a glass beaker containing 25 g of oil samples was subjected to a 20-minute treatment at 90 % power intensity. According to the results, cavitation can damage the wax crystal structure of heavy oil, reducing the viscosity. The nickel catalyst dissolves in crude oil to increase the number of active sites available and to promote polymerisation and chain-broken reaction. Furthermore, adding nickel oleate can enhance the viscosity-reducing effect by preventing resin from absorbing light components, thus increasing the number of light components.

A study by Shi et al. [101], used an ultrasonic static mixer to evaluate the decrease in viscosity of a heavy oil located in the Daqing oil field. The idea process parameters were ultrasonic power of 1.8 kW and 350 °C reaction temperature at 45 min reaction time giving a viscosity reduction rate of 57.34 %. Greater reduction in viscosity was obtained with higher ultrasonic power under the same temperature and vice versa. In addition, compared to the vis-breaking method, the ultrasonic viscosity reduction technique was more energy efficient. For processing oils of the same quality, the ultrasonic viscosity reduction method used 43.03 % less energy than the vis-breaking technology. The cavitation cracking generated some light components when the oil was stored at room temperature for 12 days. As a result, the viscosity of the residue oil did not restore to its initial level.

Doust et al. [102], examined the effects of ultrasonic irradiation duration, temperature and solvent on residue fuel oil (RFO) viscosity reduction with utilising ultrasonic irradiation being the primary focus of the study. The results demonstrated that the kinematic viscosity reduced as the temperature and solvent content increased. At ultrasonic conditions of 280 W and 24 kHz for five minutes at a temperature of 20 °C, it was discovered that the kinematic viscosity of RFO decreased from 4940 cSt to 2679 cSt. The addition of solvent during ultrasonic irradiation enhanced the promotion of API gravity and accelerated the viscosity degree (133 cSt at 50 °C and 55 by volume acetonitrile loading). The authors concluded that the examined RFO was effectively cracked and lightened by ultrasonic waves.

5.3. Chemical synthesis

The synthesis and alteration of inorganic materials has been one of the most significant uses of sonochemistry for many years [103]. Acoustic cavitation caused by high intensity ultrasonic irradiation drives bubbles to collapse which in turn cause high pressures and intense temperatures. Thus, cavitation is a way to create uncommon materials by focusing sound's diffuse energy under specific conditions. Ultrasonic techniques have drawn attention among other approaches because they can produce particles with very small sizes (2–50 nm). The process involves primary and secondary radicals that are produced during the development, expansion and violent collapse of acoustic cavity bubbles for the reduction of metals. Moreover, sonochemical methods can be combined with eco-friendly materials, giving a greener protocol [9]. Applications of sonochemistry in chemical synthesis are presented below in Fig. 16.

A work by Amulya et al. [104], synthesized nickel ferrite nanoparticles ($NiFe_2O_4$) via sonochemistry. The production of face centred cubic $NiFe_2O_4$ was confirmed by the XRD technique with a particle size ranging from 9 to 17 nm. the photocatalytic properties of the particles, when exposed to UV light, were tested using Drimarene Yellow (DY) and Methylene blue (MB) dyes demonstrating increased MB dye degradation. It was also tested for its electrochemical properties. The $NiFe_2O_4$ electrode showed a high resistance to charge transfer and a reversible electrode response. According to the findings, sonochemically synthesised $NiFe_2O_4$ nanoparticles are a good material for use in batteries,

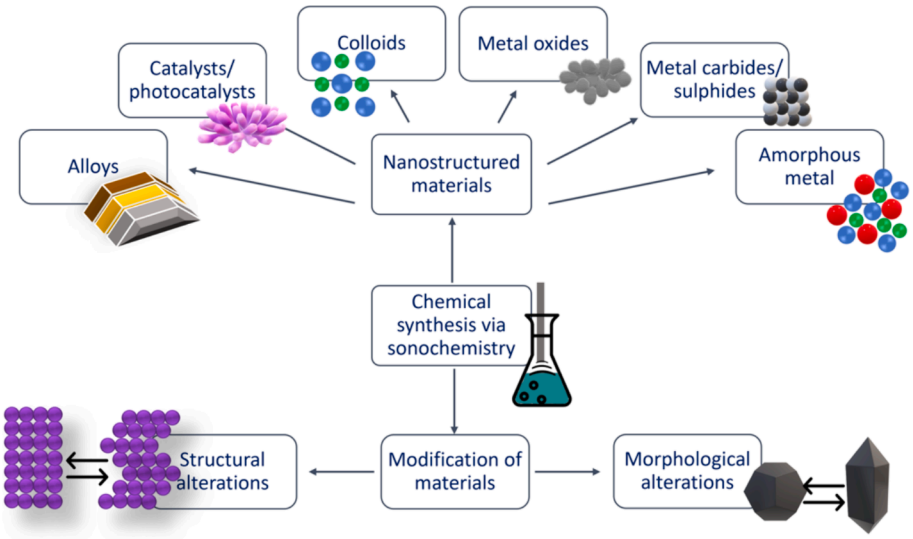

Fig. 16. Various application of sonochemistry in chemical synthesis.

sensors, energy storage devices and for the degradation of dyes.

The potential of sonochemistry as a useful tool for the deposition of gold shells on iron oxide nanoparticles (Fe_3O_4@Au, core@shell) is highlighted in a study by Dheyab et al. [105]. An ultrasonic horn was utilised with a tip size of ½ inch (20 kHz, 750 W). Based on the results, by preventing cluster agglomeration through sono-cavitation, the surface and structure of the nanoparticles was modified, leading to a more stable dispersion. Moreover, by deciphering the mechanism of synthesis of Au shell on Fe_3O_4 core nanoparticles, the sonication technology may be able to enhance the chemical activity in solution.

Zinc oxide nanoparticles (ZnO) were successfully synthesised in a single pot by Noman et al. [106], using a sonotrode of 20 kHz and 200 W. All synthesised samples contained ZnO particles with pristine hexagonal wurtzite crystalline structure, verified by various characterisation techniques and an average size three times smaller than the untreated samples. The produced ZnO nanoparticles' photocatalytic activity was assessed using MB dye. Compared to the untreated samples, the sonochemical-treated particles had stronger photocatalytic activity towards the MB dye.

Au-TiO_2 photocatalysts were produced via two different techniques-microwave and a novel sonochemistry-assisted sol–gel method- by Hernàndez et al. [107], to observe any changes in morphology and structure resulting from the energy applied to the process. The average crystallite size of the photocatalysts, obtained using the sonochemistry synthesis method, was 10.5 nm and revealed an even morphological distribution of spherical particles. In contrast, the particles synthesised via microwave technique had an average size of 8.3 nm and was increasing with the amount of Au load. Moreover, tests were conducted for the degradation of paracetamol, and it was observed that the photocatalysts synthesised via sonochemistry exhibited more promising outcomes with a superior paracetamol removal with Au content of 0.7 wt%.

A study by Monsef et al. [108], compared sonochemical-assisted method (60 W, 18 kHz) with traditional preparation methods such as hydrothermal, microwave and precipitation for the synthesis of $PrVO_4$ nanostructures. The sonochemical method was able to produce small size (39 nm) monodisperse particles using H_2 acacpn ligand. The resulting $PrVO_4$ nanostructures were used in photocatalytic degradation of organic pigments. An efficient removal of Eriochorom black T was observed at pH of 11 and catalyst amount at 0.05 g for the sonochemically and precipitation assisted $PrVO_4$ (86.92 % and 89.61 % respectively).

5.4. Crystallisation

Crystallisation is a widely utilised unit operation in the manufacturing of polymers medicines, cosmetics and solid forms of both organic and inorganic substances. However, controlling product features including morphology, polymorphism, chirality, crystal size and size distribution is challenging. The use of ultrasonography can significantly affect crystallisation and help in controlling product characteristics. The solution becomes cavitated by ultrasonic waves, improving micromixing and raising mass transfer rates. Fig. 17 depicts a proposed mechanism for how ultrasound assisted crystallisation inhibits agglomerates particles and different ultrasonic systems. These effects shorten induction time, decrease the width of the metastable zone, increase nucleation rates and reduce particle size and size distribution. However, it is necessary to solve difficulties like modelling and scale-up to increase the adaptability of this technology in the industry [109].

The impact of ultrasonic power in hen egg white lysosome (HEWL) crystallisation was investigated by Kakinouchi et al. [113], using a batch system. The samples were exposed for 10 s and 1 min of ultrasonic power (100 kHz, 100 W) at 0 and 30 min respectively. Periodically, microscopic inspections were conducted to verify the nucleation of HEWL crystals. Just after the preparation of crystallisation, ultrasonic irradiation for 10 s increased the number of nucleated crystals and the nucleation rate; however, ultrasonic irradiation for 1 min had no further effect. On the other hand, the nucleation rate was reduced by ultrasonic irradiation 30 min after crystallisation had started implying that the protein solution returned to its original state during crystallisation and that ultrasonic irradiation caused the crystal clusters to collapse.

A study conducted by Gielen et al. [110], examined sonication impacts on a commercially available activated pharmaceutical ingredient (API) to assess the technology's potential in the pharmaceutical sector. Ultrasonication was evaluated as both a substitute seeding agent and as post-treatment method to break up agglomerates. The latter approach was ineffective since only a portion of the agglomerates could be removed, and all of the crystals showed significant surface erosion. As long as enough exposure time is given, sonication during the early stages of crystallisation could prevent the production of agglomerates. The sono-treatment raised the frequency of collisions, increased the volume of particles and improved the degree of micromixing causing aggregates to break before being solidified as agglomerates. This method of precisely applying ultrasound during the seeding phase allows the adjustment of the nuclei's characteristics raising the potential of ultrasound in the pharmaceutical industry.

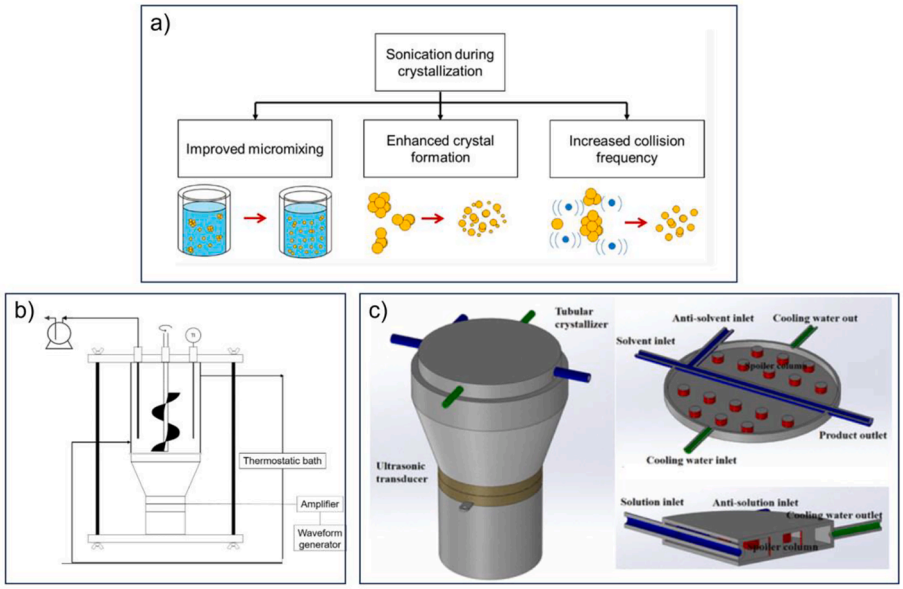

Fig. 17. a) Proposed mechanism of sonocrystallisation on the inhibition of agglomerates [110], b) NaX zeolite ultrasonic crystallisation [111] and c) crystallisation of acetylsalicylic acid in an ultrasound-assisted tube [112].

NaX zeolite was synthesised by Ramirez Mendoza et al. [111], and examined the impact of ultrasonic waves on reaction kinetics, structural and morphological characteristics. High-temperature zeolite NaX crystallisation was subjected to ultrasound utilising a plate transducer (91.8 kHz) with the irradiation moment and duration being varied. Additionally, ultrasound was used following crystallisation utilising a low-temperature horn-type transducer (20–24 kHz, 100 W/cm^2). The effects of the volume irradiated (100–300 mL), sonication duration (2–10 min) and ultrasonic power (100–200 W) were investigated. Compared to regular crystallisation, it was discovered that applying ultrasound during the first hour of crystallisation reduced reaction time by 20 %. Ultrasound can reduce the final powder's degree of agglomeration by combining high power and extended sonication time.

The effects of the crystallisation of acetylsalicylic acid on supersaturation level, ultrasonic processing duration, and power of crystallisation were investigated in a novel ultrasound-assisted tube crystallisation system designed by Zhao et al. [112], compared to previous crystallisation techniques, the ultrasonic-assisted method demonstrated superior performance in terms of better crystallisation yield, smaller particle size (8.2–40.1 μm) and narrower particle size distribution. In 0.46 s, the crystallisation efficiency reached 80 %. An alternate ultrasonic stimulation technique to speed up the crystallisation process was the pulsed ultrasound which can produce higher yields and smaller crystal sizes while maintaining a steady continuous crystallisation process at lower intensity than the continuous mode.

5.5. Wastewater treatment

Water pollution can be effectively cleaned using Advanced Oxidation Processes (AOPs). They involve UV light, Fenton reagents, sonolysis, sonocatalysis, sonophotocatalysis and have been investigated separately and in combination, with and without catalysts, for the treatment of wastewater that contains dyes, pesticides and other contaminants [114]. Ultrasound has gained popularity as a wastewater treatment technique in recent years. The intense conditions of acoustic cavitation cause water molecules and dissolved oxygen to split into • OH and O_2^{-}•. Thus, organic pollutants can break down and inorganic pollutants can oxidise in this reactive environment [115].

Membrane fouling remains one of the primary limitations of membrane ultrafiltration, despite its expanding application for wastewater treatment. Borea et al. [116], examined the use of membrane ultrafiltration in combination with ultrasound, assessing the impact of two membrane fluxes (75 and 150 L/m^2.h) as well as two ultrasound frequencies (35 and 130 kHz) on treatment efficacy and membrane fouling formation. The experimental setup is presented below (Fig. 18). The findings demonstrated that membrane ultrafiltration with ultrasound reduced membrane fouling rates to a greater extent at higher membrane flux (150 L/m^2.h) and lower ultrasound frequency used (35 kHz), with a reduction of 57.33 %, compared to the filtration process. Additionally, at a higher frequency, a greater reduction of organic waste and turbidity were noticed. The authors concluded that this combined technique can be used to improve membrane ultrafiltration and serve as a substitute for traditional tertiary wastewater treatment methods.

A study conducted by Abeledo-Lameiro et al. [117], investigated the effectiveness of ultrasonic disinfection at three different power levels, pulsed or in continuous mode, in inactivating the waterborne protozoan parasite *Cryptosporidium parvum* in simulated and experimental effluents from municipal wastewater treatment plants (MWTPs). The use of continuous mode ultrasonic irradiation at 80 W power for 10 min significantly decreased *C. parvum* vitality without changing the chemical composition of the water. Using propidium iodide, a fluorogenic vital dye, as an indicator of the integrity of the oocyst wall, higher levels of oocyst inactivation were found in MWTP effluents compared to a control solution with distilled water, regardless of the mode utilised and at 80 W. When the findings from the two modes were compared, it was evident that using the continuous mode produced far lower oocyst viability.

To determine if mechanical treatment improves sludge reduction, a study by Romero-Pareja et al. [118], used an ultrasound-assisted oxic-settling-anaerobic (OSA) method in a lab-scale wastewater treatment plant (Fig. 19). Sludge reductions of 45.72 % and 78.56 % were achieved for the two combined treatment regimes that were examined in this investigation at two different ultrasound treatment stages, UO1 and UO2. Both stages were characterised by 20 kHz frequency and 0.375 W/mL power with different energy applied (90 and 120 kJ respectively), frequency treatment and duration (3 times a day for 40 days and 4 times a day for 30 days respectively). During stage UO1, the system's overall performance and nutrient removal improved; however, stage's UO2 stronger treatment led to the opposite effect. The reduction was 10–20 % greater than that which was reported for the OSA procedure by itself

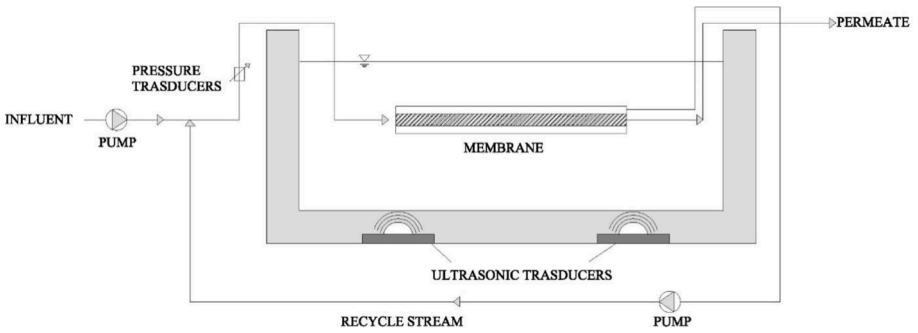

Fig. 18. Schematic illustration of the experimental device used for treating wastewater [116].

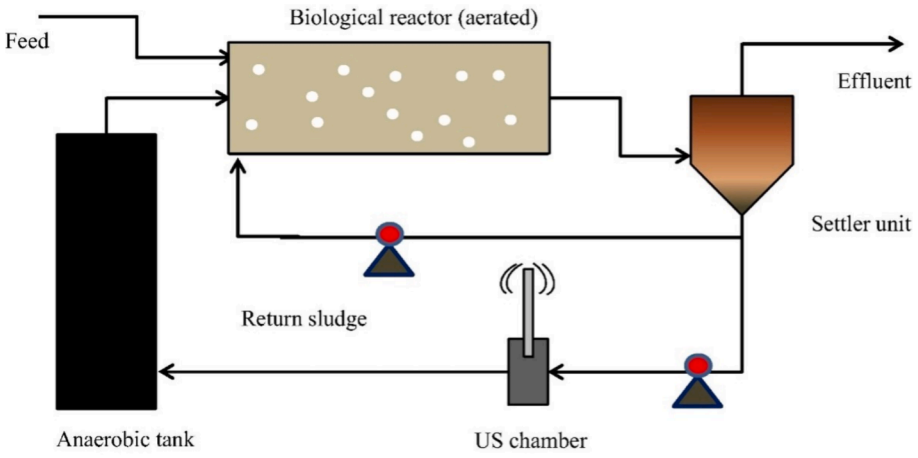

Fig. 19. Schematic representation of the lab-scale wastewater treatment plant combined with ultrasonic treatment [118].

under comparable operating parameters indicating that ultrasound helps to improve sludge removal in the OSA process.

A study to investigate the effectiveness of COD removal from olive mill wastewater (OMW) was completed by Al-Bsoul et al. [119]. The outcomes showed that the removal of COD was more effective when a combination of advanced oxidation procedures, such as ultrasound, ultraviolet irradiation and H_2O_2 were used combined with a TiO_2 catalyst than when AOPs were used alone due to the increased production of • OH radicals. The improvement of COD removal from OMW had a merely effect by the presence of H_2O_2. Maximum COD removal rate was attained using 0.75 g/L TiO_2, compared to other values studied. Higher ultrasound frequencies did not improve the COD removal rate but at lower frequencies such as 20 kHz, the removal rate was greater.

A study by Golash and Gogate [120], focused on the utilisation of sonochemical reactors for the degradation of dichlorvos in wastewater. The impact of various operational parameters and the application of various additives for potential amplification of the degradation process were investigated. In contrast to higher-frequency reactors, it was noted that low-frequency sonochemical reactors successfully treated dichlorvos pesticide. As the power intensity increased the extent of degradation increased as well due to the increased cavitational activity but this result cannot be generalised, and depending on the type of reactor, there may be an ideal power dissipation level where excessive cavitation events around the transducer cause decoupling effects. Under ideal conditions, ultrasonic cavitation and Fenton's reagent were shown to be the most efficient combination, completely eliminating the pesticide.

5.6. Extraction

Ultrasound-induced extraction is a more effective and environmentally friendly technology compared to traditional extraction methods, since it requires less solvent volume for sample preparation and takes less time to complete the extraction process (Fig. 20a). Temperature and pressure fluctuations caused by bubble implosion, when ultrasonic irradiation passes through a medium, improve the solvent's ability to permeate the matrix. As a result, the mass transfer of the analytes unto the solvent increases. Moreover, the effective sample/extractant interaction leads to good analyte recovery [121]. Furthermore, various ultrasonic reactor systems can be utilised for the sonoextraction of solid samples as depicted below in Fig. 20b. Applications for ultrasonic-assisted extraction include cosmetics, nutraceuticals, pharmaceuticals, bioenergy and the food industry [122].

The effects of ultrasonic treatments on spinach leaves throughout the extraction process were examined by Altemimi et al. [123], compared with the conventional extraction method. The varying parameters that were investigated were temperature, ultrasonic power, exposure duration and frequency. With multiple combinations, the ideal parameters for extraction yields, were an ultrasonic power of 50 % at a reaction temperature of 40 °C, an extraction period of 30 min and an ultrasonic frequency of 37 kHz. Furthermore, using ultrasonic treatment, polyphenol extraction yields from spinach increased. Because ultrasonic extraction uses less solvent and doesn't require longer extraction durations than conventional extraction, it will be less expensive to extract polyphenols from spinach.

For ultrasound-assisted liquid–liquid extraction, a novel reactor was developed by John et al. [124]. Short contact intervals were introduced for the microchannel tubing along the reactor plate to enable more concentrated ultrasonic transmission (Fig. 21). Even the non-contacted parts of the tubing were still under the influence of the ultrasound due to the pseudo-sonicated zone that the intervals created. It was found that the maximum intensities along the channel became concentrated at

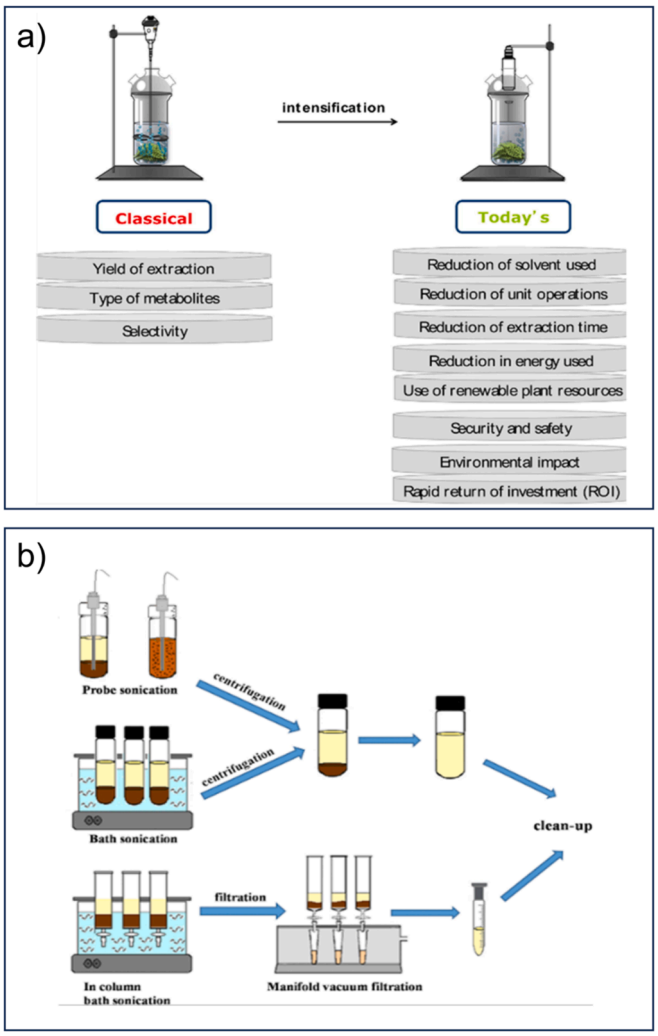

Fig. 20. a) Benefits of the ultrasonic-assisted extraction [122]. and b) different ultrasonic reactor systems for ultrasonic extraction on solid samples [121].

these intervals when comparing the thermal profiles with and without intervals. The effect of intervals was also examined on a sonicated two-phase flow, and it was observed that the emulsified aqueous phase was repeatedly divided at the intervals and coalesced, adding more interfacial area. The optimum configuration regarding the number of intervals was with five intervals and compared with a direct-contact design the mass transfer was increased by 17–29 % and the extraction yield by 13–23 %.

To maximise the ultrasonic-assisted extraction of polysaccharides from mulberry leaves a Box-Behnken design was utilised by Zhang et al. [125]. Under optimal conditions, which included an extraction temperature of 57 °C, an extraction period of 80 min and a liquid/solid ratio of 53 mL/g, the mulberry leaf polysaccharide (MLP) yield was 6.92 ± 0.29 %. Afterward, deproteinization, dialysis and decolorization were used to separate the MLPs into three fractions. The monosaccharide composition, FT-IR spectra and carbohydrate content of MPL were examined. Comparing the antioxidant activities of the three fractions, it was shown that the antioxidant activities declined as the MPL purity increased and MPLs with high concentration had relatively low antioxidant reactions.

Effective components were extracted from pomegranate peel using sono-assisted extraction technology by Sharayei et al. [126]. The yield and the antioxidant characteristics of aqueous pomegranate peel extract were examined using the response surface method in relation to independent process variables such as ultrasonic amplitude (20, 60, and 100 %) and utrasound exposure time (5, 10, and 15 min). An exposure duration of 6.2 min and 60 % of the ultrasonic amplitude were found to be the optimal conditions, based on both individual and combinations of all process variables. At these conditions, the pomegranate peel extract was predicted to have a maximum value for yield of 13.1 %. The experimental and predicted values were in good agreement.

5.7. Medicinal uses

High-intensity focused ultrasound (HIFU) is a rapidly emerging, developing technique, with a wide and important range of clinical uses. Focused ultrasound surgery (FUS), which uses HIFU to non-invasively induced tissue necrosis at a specific target, is promising for tumour ablation in the oncology area. Geometrically, focusing can be performed, either by employing a curved transducer or by utilising a flat transducer with a curved lens or with a system that uses an array of small transducers (Fig. 22). Modern transducers are capable of producing acoustic intensities of approximately 100–10000 W/cm^2, compared to diagnostic ultrasound transducers that produce intensities of 0.0001–0.1000 W/cm^2. Advances in technology and design are helping to overcome the limitations of HIFU which have postponed its further use in clinical practise. Ongoing research and experimental clinical trials are showing great potential for various types of tumours, such as renal, liver, pancreatic, breast, bone, and brain tumours [127].

Wu et al. [128], demonstrated how high-intensity focused ultrasound (HIFU) treatments affect localised breast cancer. Fig. 23 illustrates the treatment concept. Results showed that using the HIFU approach, total tumour cell necrosis is observed and concluded that the

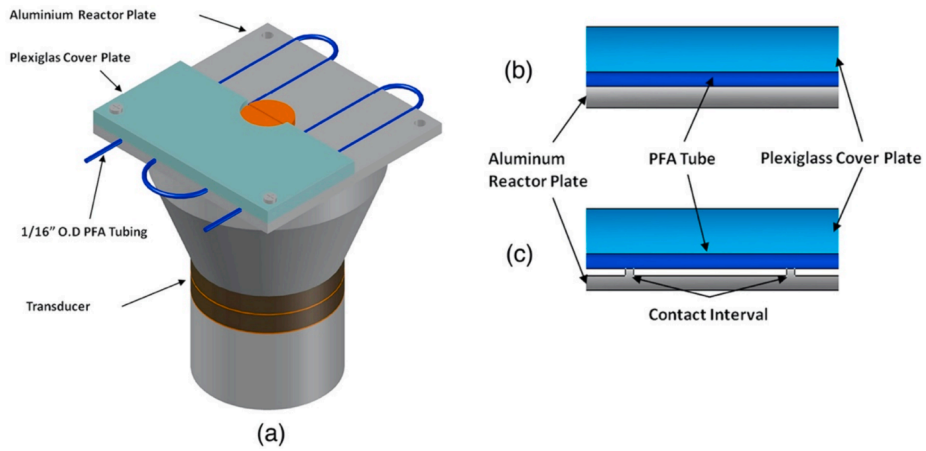

Fig. 21. Schematic illustration of a) the reactor, b) the Cross section of the direct-contact reactor, and c) the Cross section of the interval-contact reactor [124].

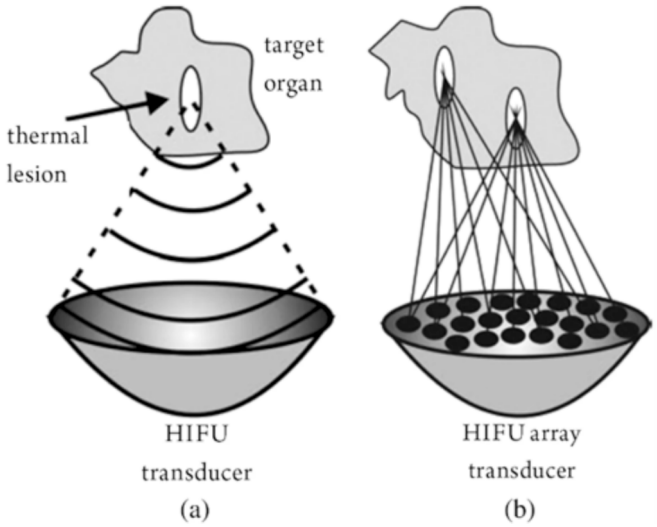

Fig. 22. A simplified illustration of a HIFU of a) a single transducer and b) array transducers [127].

HIFU method would be useful for treating breast cancer locally. However, to ascertain the future role of this method, numerous additional studies are necessary such as long-term follow-up clinical trials at larger scale that compare the long-term outcomes of HIFU treatment and breast-conserving surgery as a breast-conserving method.

A recent work by Gray et al. [129], evaluated the safety and clinical viability of employing focused ultrasound-mediated mild hyperthermia computational planning models for targeted medication administration. Ultrasound was generated by a single-element focused transducer with a frequency of 0.96 MHz varying the power from 50 to 140 W. The absence of focused ultrasound-related side effects supported the safety of the method, while the slight mean difference between the actual and model-predicted focused ultrasound powers needed to achieve hyperthermia-mediated drug delivery supported the feasibility of this method.

The purpose of a clinical trial conducted by Kotopoulis et al. [130], was to determine whether a conventional commercially available technology could be used to induce sonoporation in a clinical setting in order to improve the life quality of patients, increasing the overall survival rate of patients with pancreatic adenocarcinoma. Patients received conventional gemcitabine chemotherapy treatment and were treated for 31.5 min using an ultrasound scanner without any physical alterations was used with a centre frequency of 1.9 MHz. With this arrangement, the pancreatic tumour can be treated as the microbubbles are always present. The results showed that people with pancreatic cancer had a higher chance of surviving when ultrasound, microbubble therapy and chemotherapy were combined.

FK506-loaded microbubbles (FK506-MBs) were synthesised by Liu et al. [131], in order to release FK506 into transplanted hearts in a site-specific manner using the ultrasound-targeted microbubble destruction (UTMD) technology. The FK-506-MBs exhibited remarkable efficiency in drug loading and encapsulation, with an average particle size of 1.65 $\pm$ 0.32 μm. Lipid microbubbles were a great way to deliver medication. FK506 could be selectively supplied and locally released to transplanted heart tissues when combined with UTMD, increasing the local medication concentration while lowering systemic cytotoxic effects. Moreover, this tactic might be used to transplant rejection in other organs like kidney and liver.

6. Challenges and perspectives

Even though ultrasound technology is a “green” technology with a wide range of potential field applications and several validated outcomes from lab-scale operations, very few examples of successful sonochemical applications are carried out at the industrial scale. A major obstacle to the further development of this technology is the lack of scale-up strategies for sonoreactors to meet industrial needs. High volume operation, energy conversion, process efficiency and rates that can lead to greater treatment costs need to be taken into account when designing a sonoreactor. Moreover, due to the difficulty of accurately replicating the reactor geometry and sonochemical environment similar to laboratory-scale reactors, as well as an even distribution of cavitational activity, it is imperative to ensure that maximum efficiency can be achieved in the design of industrial-scale sonoreactors.

The key to introduce the lab-scale process to the level of industrialisation is the in-depth research and comprehension of several crucial operating parameters, such as the temperature, the frequency of ultrasound, the sonication time, the intensity of irradiation, the pressure amplitude, and the reactor design. The accomplishment of such lab-scale optimizations is a time-consuming procedure, and the implementation of mathematical and computational tools is necessary. Additionally, since sonoreactors must be designed with uniform cavitational activity to initiate a particular application, theoretical applications can be implemented. Along with the knowledge of how operating and geometric parameters affect the activity distribution, the design of a sonoreactor could be optimised. Besides that, it would be helpful to develop user-friendly computer codes in order to forecast the expected chemical effects as a function of the various operating settings, to prevent trial-and-error testing.

Industrial progress has also been delayed due to the major issues with transducer efficiency and power. In order to build transducers that

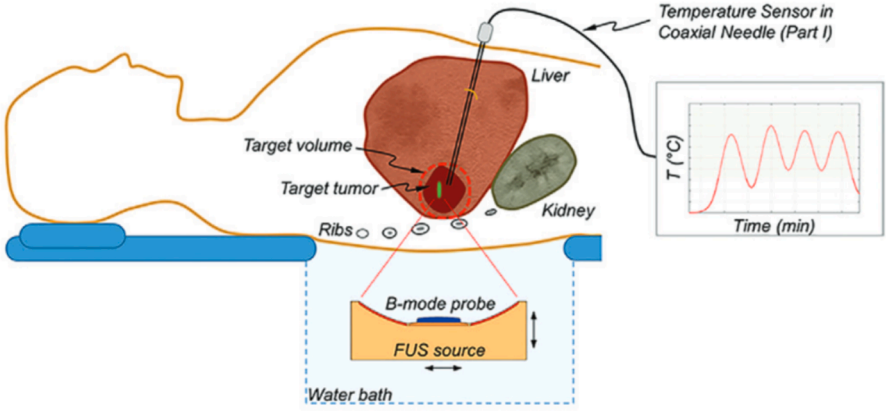

Fig. 23. Diagram of the treatment concept based on FUS [128].

operate with a high-power capacity and minimal erosion, further studies should be done. Though chemical engineers' and chemists' contributions are usually needed, the problem is mostly of a material science nature. Furthermore, a wider exposed area for the ultrasonic source, continuous flow reactor set-ups and transducer arrays are a few design improvements that need to be looked into.

Another recommendation for successfully converting the laboratory-scale technologies into commercial scale is the combination of sonochemical reactors with hydrodynamic cavitation reactors, microwaves and UV light sources to clearly demonstrate the anticipated synergism. It is also crucial to develop hybrid designs that can function both as simultaneous combination and in continuous operation at the same time. Sonoelectrochemistry, the combination of ultrasonic energy and electrochemistry, also provides a promising field in the synthesis of electrocatalysts, hydrogen, and electrodes for fuel cells with improved efficiencies and yields.

7. Conclusions

In this review, different reactor design configurations are presented pointing out their importance on the cavitation activity. Among the batch and continuous sonoreactors, the most known and utilized systems are batch sonoreactors due to their simplicity and low operating cost. Ultrasonic continuous flow sonoreactors have also intrigued the interest of the research community offering improved production rates and yields in shortened reaction times and its scalability potential. Microstructured flow sonoreactors are considered an exceptional option for continuous processes for their improved transfer phenomena due to their size. Smaller reactor sizes were found to be more efficient. Not only the optimisation of the geometry of the reactor can enhance the performance of the sonoreactor, but also the optimisation of operating parameters. The bubbles number and size as well as the temperature collapse and the yield of the reaction are interrelated with the ultrasound frequency, the irradiation intensity, and the pressure amplitude. In addition, the optimisation of sonication time and temperature is important for achieving high yields, while a further increase of sonication time or temperature could prevent the reaction and reduce the reaction rate and yield. The classification of sonochemistry as an environmentally friendly method and due to the physical forces and chemical reactions occurring within the sonoreactors, a wide range of applications has been developed. Applications that are implemented so far include the improvement of microbial cell disruption, the upgrade of the quality of crude oil and residues and the particle synthesis achieving small sizes. Moreover, the control of product features and characteristics of polymer medicine and cosmetics, the wastewater treatment and the extraction were found to be more effective processes. Sonochemistry can also be involved in medicinal uses developing promising techniques in the oncology area. The advantages that sonochemistry offers in different applications outweigh, the struggles of operating larger volumes at pilot and industrial level must overcome. Developing computational tools to carry out theoretical investigations is a key factor for the efficient optimisation of the design and the operating parameters of the sonoreactors.

CRediT authorship contribution statement

Panayiota Adamou: Writing – review & editing, Writing – original draft, Formal analysis, Data curation. **Eleana Harkou:** Writing – review & editing, Writing – original draft, Formal analysis, Data curation. **Alberto Villa:** Writing – review & editing, Writing – original draft, Visualization. **Achilleas Constantinou:** Writing – review & editing, Writing – original draft, Visualization, Supervision, Conceptualization. **Nikolaos Dimitratos:** Writing – review & editing, Writing – original draft, Visualization, Supervision, Conceptualization.

Declaration of competing interest

The authors declare that they have no known competing financial interests or personal relationships that could have appeared to influence the work reported in this paper.

Data availability

No data was used for the research described in the article.

References

[1] S.K. Bhangu, M. Ashokkumar, Theory of Sonochemistry, in: J.C. Colmenares, G. Chatel (Eds.), Sonochemistry: from Basic Principles to Innovative Applications, Springer International Publishing, Cham, 2017, pp. 1–28, https://doi.org/10.1007/978-3-319-54271-3_1.
[2] J. Luo, Z. Fang, R.L. Smith, X. Qi, Fundamentals of Acoustic Cavitation in Sonochemistry, in Production of Biofuels and Chemicals with Ultrasound, Z. Fang, Jr. Smith Richard L., and X. Qi, Eds., Dordrecht: Springer Netherlands, 2015, pp. 3–33. doi: 10.1007/978-94-017-9624-8_1.
[3] I.V. Machado, J.R.N. dos Santos, M.A.P. Januario, A.G. Corrêa, Greener organic synthetic methods: sonochemistry and heterogeneous catalysis promoted multicomponent reactions, Ultrason. Sonochem. 78 (Oct. 2021) 105704, https://doi.org/10.1016/j.ultsonch.2021.105704.
[4] R. Mettin, C. Cairós, A. Troia, Sonochemistry and bubble dynamics, Ultrason. Sonochem. 25 (Jul. 2015) 24–30, https://doi.org/10.1016/j.ultsonch.2014.08.015.
[5] P.R. Gogate, P.N. Patil, Sonochemical Reactors, in: J.C. Colmenares, G. Chatel (Eds.), Sonochemistry: from Basic Principles to Innovative Applications, Springer International Publishing, Cham, 2017, pp. 255–281, https://doi.org/10.1007/978-3-319-54271-3_10.
[6] Z. Dong, C. Delacour, K. Mc Carogher, A.P. Udepurkar, S. Kuhn, Continuous ultrasonic reactors: design, mechanism and application, Materials 13 (2) (2020), https://doi.org/10.3390/ma13020344.
[7] S. Asgharzadehahmadi, A.A. Abdul Raman, R. Parthasarathy, B. Sajjadi, Sonochemical reactors: review on features, advantages and limitations, Renew. Sustain. Energ. Rev. 63 (2016) 302–314, https://doi.org/10.1016/j.rser.2016.05.030.
[8] P. Adamou, et al., Recent progress on sonochemical production for the synthesis of efficient photocatalysts and the impact of reactor design, Ultrason. Sonochem. 100 (Nov. 2023) 106610, https://doi.org/10.1016/j.ultsonch.2023.106610.
[9] B. Savun-Hekimoğlu, A review on sonochemistry and its environmental applications, Acoustics 2 (4) (2020) 766–775, https://doi.org/10.3390/acoustics2040042.
[10] P.R. Gogate, A.B. Pandit, Sonophotocatalytic reactors for wastewater treatment: a critical review, AIChE J 50 (5) (May 2004) 1051–1079, https://doi.org/10.1002/aic.10079.
[11] P. Gupta, S. Suresh, J.M. Jha, F. Banat, M. Sillanpää, Sonochemical degradation of polycyclic aromatic hydrocarbons: a review, Environ. Chem. Lett. 19 (3) (Jun. 2021) 2663–2687, https://doi.org/10.1007/s10311-020-01157-9.
[12] M.H. Dehghani, et al., Recent trends in the applications of sonochemical reactors as an advanced oxidation process for the remediation of microbial hazards associated with water and wastewater: a critical review, Ultrason. Sonochem. 94 (Mar. 2023) 106302, https://doi.org/10.1016/j.ultsonch.2023.106302.
[13] M. Pirsaheb, N. Moradi, H. Hossini, Sonochemical processes for antibiotics removal from water and wastewater: a systematic review, Chem. Eng. Res. Des. 189 (Jan. 2023) 401–439, https://doi.org/10.1016/j.cherd.2022.11.019.
[14] N.S.M. Yusof, S. Anandan, P. Sivashanmugam, E.M.M. Flores, M. Ashokkumar, A correlation between cavitation bubble temperature, sonoluminescence and interfacial chemistry – a minireview, Ultrason. Sonochem. 85 (Apr. 2022) 105988, https://doi.org/10.1016/j.ultsonch.2022.105988.
[15] Y.G. Adewuyi, Sonochemistry: environmental science and engineering applications, Ind. Eng. Chem. Res. 40 (22) (Oct. 2001) 4681–4715, https://doi.org/10.1021/ie010096l.
[16] X. Li, Y. Song, Z. Hao, C. Gu, Cavitation mechanism of oil-film bearing and development of a new gaseous cavitation model based on air solubility, J. Tribol. 134 (031701) (2012), https://doi.org/10.1115/1.4006702.
[17] S. Xu, J. Wang, B. Cai, H. Cheng, B. Ji, Z. Zhang, X. Long, Investigation on cavitation initiation in jet pump cavitation reactors with special emphasis on two mechanisms of cavitation initiation, Physics of Fluids 34 (1) (2022) 013308, https://doi.org/10.1063/5.0075099.
[18] X. Cheng, K. Yang, J. Wang, W. Xiao, S. Huang, Ultrasonic system and ultrasonic metal welding performance: a status review, J. Manuf. Process. 84 (2022) 1196–1216.
[19] J. Chen, et al., A review of ultrahigh frequency ultrasonic transducers, Front. Mater. 8 (Jan. 2022) 733358, https://doi.org/10.3389/fmats.2021.733358.
[20] L. Yusuf, M.D. Symes, P. Prentice, Characterising the cavitation activity generated by an ultrasonic horn at varying tip-vibration amplitudes, Ultrason. Sonochem. 70 (Jan. 2021) 105273, https://doi.org/10.1016/j.ultsonch.2020.105273.
[21] K. Zhang, G. Gao, C. Zhao, Y. Wang, Y. Wang, J. Li, Review of the design of power ultrasonic generator for piezoelectric transducer, Ultrason. Sonochem. 96 (Jun. 2023) 106438, https://doi.org/10.1016/j.ultsonch.2023.106438.

[22] V.S. Sutkar, P.R. Gogate, Design aspects of sonochemical reactors: techniques for understanding cavitational activity distribution and effect of operating parameters, Chem. Eng. J. 155 (1) (Dec. 2009) 26–36, https://doi.org/10.1016/j.cej.2009.07.021.
[23] Y. Asakura, K. Yasuda, Study on the efficiency of a transducer for sonochemistry by calorimetry, Japanese J. Appl. Phys. 61 (SG) (2022) SG1032, https://doi.org/10.35848/1347-4065/ac4820.
[24] K. Srathonghuam, B. Wonganu, W. Busayaporn, J. Thongsri, Vibration analysis and development of a submersible ultrasonic transducer for an application in the inhibitory activity of pathogenic bacteria, IEEE Access 9 (2021) 142362–142373.
[25] A.A. Vjuginova, Multifrequency langevin-type ultrasonic transducer, Russ. J. Nondestr. Test. 55 (4) (Apr. 2019) 249–254, https://doi.org/10.1134/S1061830919040132.
[26] V.D. Luong et al., Measuring the vibration amplitude of the ultrasonic transducer. 2021.
[27] X. Lu, J. Hu, H. Peng, Y. Wang, A new topological structure for the Langevin-type ultrasonic transducer, Ultrasonics 75 (Mar. 2017) 1–8, https://doi.org/10.1016/j.ultras.2016.11.008.
[28] R.J. Wood, A. Bertin, J. Lee, M.J. Bussemaker, The application of flow to an ultrasonic horn system: phenol degradation and sonoluminescence, Ultrason. Sonochem. 71 (Mar. 2021) 105373, https://doi.org/10.1016/j.ultsonch.2020.105373.
[29] S. Kumar, C.S. Wu, G.K. Padhy, W. Ding, Application of ultrasonic vibrations in welding and metal processing: A status review, J. Manuf. Process. 26 (Apr. 2017) 295–322, https://doi.org/10.1016/j.jmapro.2017.02.027.
[30] P. Kumar, K. Prakasan, Acoustic horn design for joining metallic wire with flat metallic sheet by ultrasonic vibrations, Journal of Vibroengineering 20 (7) (Nov. 2018) 2758–2770, https://doi.org/10.21595/jve.2018.19648.
[31] Y. Son, M. Lim, J. Khim, Investigation of acoustic cavitation energy in a large-scale sonoreactor, Ultrason. Sonochem. 16 (4) (Apr. 2009) 552–556, https://doi.org/10.1016/j.ultsonch.2008.12.004.
[32] Y. Son, Y. No, J. Kim, Geometric and operational optimization of 20-kHz probe-type sonoreactor for enhancing sonochemical activity, Ultrason. Sonochem. 65 (Jul. 2020) 105065, https://doi.org/10.1016/j.ultsonch.2020.105065.
[33] M. Lim, M. Ashokkumar, Y. Son, The effects of liquid height/volume, initial concentration of reactant and acoustic power on sonochemical oxidation, Ultrason. Sonochem. 21 (6) (Nov. 2014) 1988–1993, https://doi.org/10.1016/j.ultsonch.2014.03.005.
[34] K.V.B. Tran, Y. Asakura, S. Koda, Influence of liquid height on mechanical and chemical effects in 20 kHz sonication, Japanese J. Appl. Phys. 52 (7S) (2013) 07HE07, https://doi.org/10.7567/JJAP.52.07HE07.
[35] Y. Asakura, T. Nishida, T. Matsuoka, S. Koda, Effects of ultrasonic frequency and liquid height on sonochemical efficiency of large-scale sonochemical reactors, Ultrason. Sonochem. 15 (3) (Mar. 2008) 244–250, https://doi.org/10.1016/j.ultsonch.2007.03.012.
[36] Y. Asakura, S. Fukutomi, K. Yasuda, S. Koda, Optimization of sonochemical reactors by measuring impedance of transducer and sound pressure in solution, J. Chem. Eng. Jpn. 43 (12) (2010) 1008–1013.
[37] D. Kobayashi, H. Matsumoto, C. Kuroda, Effect of reactor's positions on polymerization and degradation in an ultrasonic field, Ultrason. Sonochem. 15 (3) (Mar. 2008) 251–256, https://doi.org/10.1016/j.ultsonch.2007.04.001.
[38] D. Kobayashi, K. Sano, Y. Takeuchi, K. Terasaka, Effect of irradiation distance on degradation of phenol using indirect ultrasonic irradiation method, Ultrason. Sonochem. 18 (5) (Sep. 2011) 1205–1210, https://doi.org/10.1016/j.ultsonch.2011.01.010.
[39] J.A. Kewalramani, B. Bezerra de Souza, R.W. Marsh, J.N. Meegoda, Contributions of reactor geometry and ultrasound frequency on the efficiency of sonochemical reactor, Ultrason. Sonochem. 98 (Aug. 2023) 106529, https://doi.org/10.1016/j.ultsonch.2023.106529.
[40] D. Lee, J. Kang, Y. Son, Effect of violent mixing on sonochemical oxidation activity under various geometric conditions in 28-kHz sonoreactor, Ultrason. Sonochem. 101 (Dec. 2023) 106659, https://doi.org/10.1016/j.ultsonch.2023.106659.
[41] S. Rodrigues, F.A.N. Fernandes, E.S. de Brito, A.D. Sousa, N. Narain, Ultrasound extraction of phenolics and anthocyanins from jabuticaba peel, Ind. Crop. Prod. 69 (Jul. 2015) 400–407, https://doi.org/10.1016/j.indcrop.2015.02.059.
[42] Y. Son, Simple design strategy for bath-type high-frequency sonoreactors, Chem. Eng. J. 328 (Nov. 2017) 654–664, https://doi.org/10.1016/j.cej.2017.07.012.
[43] A. Alsalme, A. AlFawaz, A.H. Glal, M.F. Abdel Messih, A. Soltan, M.A. Ahmed, S-scheme AgIO4/CeO2 heterojunction nanocomposite photocatalyst for degradation of rhodamine B dye, Journal of Photochemistry and Photobiology A: Chemistry, vol. 439, p. 114596, May 2023, doi: 10.1016/j.jphotochem.2023.114596.
[44] K. Kaviyarasan, V. Vinoth, T. Sivasankar, A.M. Asiri, J.J. Wu, S. Anandan, Photocatalytic and photoelectrocatalytic performance of sonochemically synthesized Cu2O@TiO2 heterojunction nanocomposites, Ultrason. Sonochem. 51 (Mar. 2019) 223–229, https://doi.org/10.1016/j.ultsonch.2018.10.022.
[45] A.V. Mohod, P.R. Gogate, Improved crystallization of ammonium sulphate using ultrasound assisted approach with comparison with the conventional approach, Ultrason. Sonochem. 41 (Mar. 2018) 310–318, https://doi.org/10.1016/j.ultsonch.2017.09.047.
[46] S.S. Gandhi, P.R. Gogate, Process intensification of fatty acid ester production using esterification followed by transesterification of high acid value mahua (lluppai ennai) oil: comparison of the ultrasonic reactors, Fuel 294 (Jun. 2021) 120560, https://doi.org/10.1016/j.fuel.2021.120560.
[47] S.S. Rashwan, I. Dincer, A. Mohany, Investigation of acoustic and geometric effects on the sonoreactor performance, Ultrason. Sonochem. 68 (Nov. 2020) 105174, https://doi.org/10.1016/j.ultsonch.2020.105174.
[48] C.A. Bizzi, D. Santos, T.C. Sieben, G.V. Motta, P.A. Mello, E.M.M. Flores, Furfural production from lignocellulosic biomass by ultrasound-assisted acid hydrolysis, Ultrason. Sonochem. 51 (Mar. 2019) 332–339, https://doi.org/10.1016/j.ultsonch.2018.09.011.
[49] D. Santos, U.F. Silva, F.A. Duarte, C.A. Bizzi, E.M.M. Flores, P.A. Mello, Ultrasound-assisted acid hydrolysis of cellulose to chemical building blocks: application to furfural synthesis, Ultrason. Sonochem. 40 (Jan. 2018) 81–88, https://doi.org/10.1016/j.ultsonch.2017.04.034.
[50] M. Zargazi, M.H. Entezari, Sonochemical versus hydrothermal synthesis of bismuth tungstate nanostructures: photocatalytic, sonocatalytic and sonophotocatalytic activities, Ultrason. Sonochem. 51 (Mar. 2019) 1–11, https://doi.org/10.1016/j.ultsonch.2018.10.010.
[51] B. Palanisamy, B. Paul, C. Chang, The synthesis of cadmium sulfide nanoplatelets using a novel continuous flow sonochemical reactor, Ultrason. Sonochem. 26 (Sep. 2015) 452–460, https://doi.org/10.1016/j.ultsonch.2015.01.004.
[52] E. Loranger, M. Paquin, C. Daneault, B. Chabot, Comparative study of sonochemical effects in an ultrasonic bath and in a large-scale flow-through sonoreactor, Chem. Eng. J. 178 (Dec. 2011) 359–365, https://doi.org/10.1016/j.cej.2011.10.021.
[53] A. Shamseddini, D. Mowla, F. Esmaeilzadeh, Continuous treatment of petroleum products in a tailor-made flow-through sonoreactor, J. Pet. Sci. Eng. 173 (Feb. 2019) 1149–1162, https://doi.org/10.1016/j.petrol.2018.10.068.
[54] T. Lippert, J. Bandelin, A. Musch, J.E. Drewes, K. Koch, Energy-positive sewage sludge pre-treatment with a novel ultrasonic flatbed reactor at low energy input, Bioresour. Technol. 264 (Sep. 2018) 298–305, https://doi.org/10.1016/j.biortech.2018.05.073.
[55] T. Lippert, J. Bandelin, F. Schlederer, J.E. Drewes, K. Koch, Impact of ultrasound-induced cavitation on the fluid dynamics of water and sewage sludge in ultrasonic flatbed reactors, Ultrason. Sonochem. 55 (Jul. 2019) 217–222, https://doi.org/10.1016/j.ultsonch.2019.01.024.
[56] A. Kumar, P.R. Gogate, A.B. Pandit, Mapping the efficacy of new designs for large scale sonochemical reactors, Ultrason. Sonochem. 14 (5) (Jul. 2007) 538–544, https://doi.org/10.1016/j.ultsonch.2006.11.005.
[57] J.C. Colmenares, V. Nair, E. Kuna, D. Łomot, Development of photocatalyst coated fluoropolymer based microreactor using ultrasound for water remediation, Ultrason. Sonochem. 41 (Mar. 2018) 297–302, https://doi.org/10.1016/j.ultsonch.2017.09.053.
[58] K. Thangavadivel, M. Konagaya, K. Okitsu, M. Ashokkumar, Ultrasound-assisted degradation of methyl orange in a micro reactor, J. Environ. Chem. Eng. 2 (3) (Sep. 2014) 1841–1845, https://doi.org/10.1016/j.jece.2014.08.004.
[59] P.R. Gogate, V.S. Sutkar, A.B. Pandit, Sonochemical reactors: Important design and scale up considerations with a special emphasis on heterogeneous systems, Chem. Eng. J. 166 (3) (Feb. 2011) 1066–1082, https://doi.org/10.1016/j.cej.2010.11.069.
[60] A. Esmaeili, M.H. Entezari, Facile and fast synthesis of graphene oxide nanosheets via bath ultrasonic irradiation, J. Colloid Interface Sci. 432 (Oct. 2014) 19–25, https://doi.org/10.1016/j.jcis.2014.06.055.
[61] S. Fukunaga, et al., Effect of geometrical configuration of reactor on a ZrP nano-dispersion process using ultrasonic irradiation, Ultrason. Sonochem. 52 (Apr. 2019) 157–163, https://doi.org/10.1016/j.ultsonch.2018.11.008.
[62] Y. Son, M. Lim, M. Ashokkumar, J. Khim, Geometric optimization of sonoreactors for the enhancement of sonochemical activity, J. Phys. Chem. C 115 (10) (Mar. 2011) 4096–4103, https://doi.org/10.1021/jp110319y.
[63] V. Vargas, L. Marczak, S. Flôres, G. Mercali, Advanced technologies applied to enhance properties and structure of films and coatings: a review, Food Bioproc. Tech. 15 (Jun. 2022), https://doi.org/10.1007/s11947-022-02768-6.
[64] P.R. Gogate, Cavitational reactors for process intensification of chemical processing applications: a critical review, Chem. Eng. Process. 47 (4) (Apr. 2008) 515–527, https://doi.org/10.1016/j.cep.2007.09.014.
[65] T.J. Mason, A. Collings, A. Sumel, Sonic and ultrasonic removal of chemical contaminants from soil in the laboratory and on a large scale, Ultrason. Sonochem. 11 (3) (May 2004) 205–210, https://doi.org/10.1016/j.ultsonch.2004.01.025.
[66] S. Kentish, H. Feng, Applications of power ultrasound in food processing, Annu. Rev. Food Sci. Technol. 5 (2014) 263–284.
[67] L.S. Teixeira, H.P. Vieira, C.C. Windmöller, C.C. Nascentes, Fast determination of trace elements in organic fertilizers using a cup-horn reactor for ultrasound-assisted extraction and fast sequential flame atomic absorption spectrometry, Talanta 119 (Feb. 2014) 232–239, https://doi.org/10.1016/j.talanta.2013.11.018.
[68] K.A. Ramisetty, A.B. Pandit, P.R. Gogate, Ultrasound assisted preparation of emulsion of coconut oil in water: understanding the effect of operating parameters and comparison of reactor designs, Chem. Eng. Process. 88 (Feb. 2015) 70–77, https://doi.org/10.1016/j.cep.2014.12.006.
[69] P.R. Gogate, A.L. Prajapat, Depolymerization using sonochemical reactors: a critical review, Ultrason. Sonochem. 27 (Nov. 2015) 480–494, https://doi.org/10.1016/j.ultsonch.2015.06.019.
[70] D. Meroni, R. Djellabi, M. Ashokkumar, C.L. Bianchi, D.C. Boffito, Sonoprocessing: from concepts to large-scale reactors, Chem. Rev. 122 (3) (Feb. 2022) 3219–3258, https://doi.org/10.1021/acs.chemrev.1c00438.
[71] S. Rashmi Pradhan, R.F. Colmenares-Quintero, J.C. Colmenares Quintero, Designing microflowreactors for photocatalysis using sonochemistry: a systematic

review article, Molecules, vol. 24, no. 18, 2019, doi: 10.3390/molecules24183315.
[72] V.V. Banakar, S.S. Sabnis, P.R. Gogate, A. Raha, Saurabh, Ultrasound assisted continuous processing in microreactors with focus on crystallization and chemical synthesis: A critical review, Chem. Eng. Res. Desig. vol. 182, pp. 273–289, Jun. 2022, doi: 10.1016/j.cherd.2022.03.049.
[73] R.J. Wood, J. Lee, M.J. Bussemaker, A parametric review of sonochemistry: control and augmentation of sonochemical activity in aqueous solutions, Ultrason. Sonochem. 38 (Sep. 2017) 351–370, https://doi.org/10.1016/j.ultsonch.2017.03.030.
[74] D.M. Montoya-Rodríguez, E.A. Serna-Galvis, F. Ferraro, R.A. Torres-Palma, Degradation of the emerging concern pollutant ampicillin in aqueous media by sonochemical advanced oxidation processes - parameters effect, removal of antimicrobial activity and pollutant treatment in hydrolyzed urine, J. Environ. Manage. 261 (May 2020) 110224, https://doi.org/10.1016/j.jenvman.2020.110224.
[75] F. Bößl, et al., Effect of frequency and power on the piezocatalytic and sonochemical degradation of dyes in water, Chemical Engineering Journal Advances 14 (May 2023) 100477, https://doi.org/10.1016/j.ceja.2023.100477.
[76] K. Kerboua, O. Hamdaoui, A. Alghyamah, Acoustic frequency and optimum sonochemical production at single and multi-bubble scales: a modeling answer to the scaling dilemma, Ultrason. Sonochem. 70 (Jan. 2021) 105341, https://doi.org/10.1016/j.ultsonch.2020.105341.
[77] N.E. Chadi, S. Merouani, O. Hamdaoui, M. Bouhelassa, New aspect of the effect of liquid temperature on sonochemical degradation of nonvolatile organic pollutants in aqueous media, Separation and Purification Technology 200 (Jul. 2018) 68–74, https://doi.org/10.1016/j.seppur.2018.01.047.
[78] P. Wang, C. Cheng, Y. Ma, M. Jia, Degradation behavior of polyphenols in model aqueous extraction system based on mechanical and sonochemical effects induced by ultrasound, Sep. Purif. Technol. 247 (Sep. 2020) 116967, https://doi.org/10.1016/j.seppur.2020.116967.
[79] L. Yuan, T. Wang, F. Xing, X. Wang, H. Yun, Enhancement of Anammox performances in an ABR at normal temperature by the low-intensity ultrasonic irradiation, Ultrason. Sonochem. 73 (May 2021) 105468, https://doi.org/10.1016/j.ultsonch.2021.105468.
[80] S.S. Nadar, V.K. Rathod, Sonochemical effect on activity and conformation of commercial lipases, Appl. Biochem. Biotechnol. 181 (4) (Apr. 2017) 1435–1453, https://doi.org/10.1007/s12010-016-2294-2.
[81] S.M. Joshi, P.R. Gogate, Intensifying the biogas production from food waste using ultrasound: understanding into effect of operating parameters, Ultrason. Sonochem. 59 (Dec. 2019) 104755, https://doi.org/10.1016/j.ultsonch.2019.104755.
[82] M.M. Ghafurian, Z. Akbari, H. Niazmand, R. Mehrkhah, S. Wongwises, O. Mahian, Effect of sonication time on the evaporation rate of seawater containing a nanocomposite, Ultrason. Sonochem. 61 (Mar. 2020) 104817, https://doi.org/10.1016/j.ultsonch.2019.104817.
[83] Y. Asakura, K. Yasuda, Frequency and power dependence of ultrasonic degassing, Ultrason. Sonochem. 82 (Jan. 2022) 105890, https://doi.org/10.1016/j.ultsonch.2021.105890.
[84] J.-C. Lin, S.-L. Lo, C.-Y. Hu, Y.-C. Lee, J. Kuo, Enhanced sonochemical degradation of perfluorooctanoic acid by sulfate ions, Ultrason. Sonochem. 22 (Jan. 2015) 542–547, https://doi.org/10.1016/j.ultsonch.2014.06.006.
[85] J.A. Fuentes-García, J. Santoyo-Salzar, E. Rangel-Cortes, G.F. Goya, V. Cardozo-Mata, J.A. Pescador-Rojas, Effect of ultrasonic irradiation power on sonochemical synthesis of gold nanoparticles, Ultrason. Sonochem. 70 (Jan. 2021) 105274, https://doi.org/10.1016/j.ultsonch.2020.105274.
[86] T. Yamamoto, S. Hatanaka, S.V. Komarov, Fragmentation of cavitation bubble in ultrasound field under small pressure amplitude, Ultrason. Sonochem. 58 (Nov. 2019) 104684, https://doi.org/10.1016/j.ultsonch.2019.104684.
[87] T. Yamamoto, S.V. Komarov, Enhancement of oscillation amplitude of cavitation bubble due to acoustic wake effect in multibubble environment, Ultrason. Sonochem. 78 (Oct. 2021) 105734, https://doi.org/10.1016/j.ultsonch.2021.105734.
[88] A. Afzal, I. Nawfal, I.M. Mahbubul, S.S. Kumbar, An overview on the effect of ultrasonication duration on different properties of nanofluids, J. Therm. Anal. Calorim. 135 (1) (Jan. 2019) 393–418, https://doi.org/10.1007/s10973-018-7144-8.
[89] F.E. Yunita, N.C. Natasha, E. Sulistiyono, A.R. Rhamdani, A. Hadinata, E. Yustanti, Time and amplitude effect on nano magnesium oxide synthesis from bittern using sonochemical process, IOP Conference Series: Materials Science and Engineering 858 (1) (Jun. 2020) 012045, https://doi.org/10.1088/1757-899X/858/1/012045.
[90] G.B. Daware, P.R. Gogate, Sonochemical degradation of 3-methylpyridine (3MP) intensified using combination with various oxidants, Ultrason. Sonochem. 67 (Oct. 2020) 105120, https://doi.org/10.1016/j.ultsonch.2020.105120.
[91] C.H. Han, B.G. Min, Superhydrophobic and antibacterial properties of cotton fabrics coated with copper nanoparticles through sonochemical process, Fibers Polym. 21 (4) (Apr. 2020) 785–791, https://doi.org/10.1007/s12221-020-9925-5.
[92] Y. Liu, M. Li, Y. Liu, F. Bai, K. Bian, Effects of pulsed ultrasound at 20 kHz on the sonochemical degradation of mycotoxins, World Mycotoxin J. 12 (4) (2019) 357–366.
[93] P.R. Gogate, A.M. Kabadi, A review of applications of cavitation in biochemical engineering/biotechnology, Biochem. Eng. J. 44 (1) (Apr. 2009) 60–72, https://doi.org/10.1016/j.bej.2008.10.006.
[94] Z. Liu, S. Smith, Enzyme recovery from biological wastewater treatment, Waste Biomass Valoriz. 12 (Aug. 2021), https://doi.org/10.1007/s12649-020-01251-7.
[95] A.Z. Sulaiman, A. Ajit, R.M. Yunus, Y. Chisti, Ultrasound-assisted fermentation enhances bioethanol productivity, Biochem. Eng. J. 54 (3) (May 2011) 141–150, https://doi.org/10.1016/j.bej.2011.01.006.
[96] M. Wang, W. Yuan, X. Jiang, Y. Jing, Z. Wang, Disruption of microalgal cells using high-frequency focused ultrasound, Bioresour. Technol. 153 (Feb. 2014) 315–321, https://doi.org/10.1016/j.biortech.2013.11.054.
[97] K. Yamamoto, P.M. King, X. Wu, T.J. Mason, E.M. Joyce, Effect of ultrasonic frequency and power on the disruption of algal cells, Ultrason. Sonochem. 24 (May 2015) 165–171, https://doi.org/10.1016/j.ultsonch.2014.11.002.
[98] M. Kurokawa, P.M. King, X. Wu, E.M. Joyce, T.J. Mason, K. Yamamoto, Effect of sonication frequency on the disruption of algae, Ultrason. Sonochem. 31 (Jul. 2016) 157–162, https://doi.org/10.1016/j.ultsonch.2015.12.011.
[99] J. Cui, Z. Zhang, X. Liu, L. Liu, J. Peng, Studies on viscosity reduction and structural change of crude oil treated with acoustic cavitation, Fuel 263 (Mar. 2020) 116638, https://doi.org/10.1016/j.fuel.2019.116638.
[100] A.N. Sawarkar, A.B. Pandit, S.D. Samant, J.B. Joshi, Use of ultrasound in petroleum residue upgradation, Can. J. Chem. Eng. 87 (3) (Jun. 2009) 329–342, https://doi.org/10.1002/cjce.20169.
[101] C. Shi, et al., Application and mechanism of ultrasonic static mixer in heavy oil viscosity reduction, Ultrason. Sonochem. 37 (Jul. 2017) 648–653, https://doi.org/10.1016/j.ultsonch.2017.02.027.
[102] A.M. Doust, M. Rahimi, M. Feyzi, Effects of solvent addition and ultrasound waves on viscosity reduction of residue fuel oil, Chem. Eng. Process. 95 (Sep. 2015) 353–361, https://doi.org/10.1016/j.cep.2015.07.014.
[103] K.S. Suslick, M.M. Fang, T. Hyeon, M.M. Mdleleni, Applications of Sonochemistry to Materials Synthesis, in Sonochemistry and Sonoluminescence, L.A. Crum, T.J. Mason, J.L. Reisse, K.S. Suslick, Eds., Dordrecht: Springer Netherlands, 1999, pp. 291–320. doi: 10.1007/978-94-015-9215-4_24.
[104] M.A.S. Amulya, H.P. Nagaswarupa, M.R.A. Kumar, C.R. Ravikumar, S. C. Prashantha, K.B. Kusuma, Sonochemical synthesis of NiFe2O4 nanoparticles: characterization and their photocatalytic and electrochemical applications, Appl. Surf. Sci. Adv. 1 (Nov. 2020) 100023, https://doi.org/10.1016/j.apsadv.2020.100023.
[105] M.A. Dheyab, A.A. Aziz, M.S. Jameel, P.M. Khaniabadi, B. Mehrdel, Mechanisms of effective gold shell on Fe3O4 core nanoparticles formation using sonochemistry method, Ultrason. Sonochem. 64 (Jun. 2020) 104865, https://doi.org/10.1016/j.ultsonch.2019.104865.
[106] M.T. Noman, M. Petru, J. Militký, M. Azeem, M.A. Ashraf, One-Pot sonochemical synthesis of ZnO nanoparticles for photocatalytic applications modelling and optimization, Materials 13 (1) (2020) pp, https://doi.org/10.3390/ma13010014.
[107] R. Hernández, et al., Au-TiO2 synthesized by a microwave- and sonochemistry-assisted sol-gel method: characterization and application as photocatalyst, Catalysts 10 (9) (2020) pp, https://doi.org/10.3390/catal10091052.
[108] R. Monsef, M. Ghiyasiyan-Arani, O. Amiri, M. Salavati-Niasari, Sonochemical synthesis, characterization and application of PrVO4 nanostructures as an effective photocatalyst for discoloration of organic dye contaminants in wastewater, Ultrason. Sonochem. 61 (Mar. 2020) 104822, https://doi.org/10.1016/j.ultsonch.2019.104822.
[109] R. Prasad, S.V. Dalvi, Sonocrystallization: monitoring and controlling crystallization using ultrasound, Chem. Eng. Sci. 226 (Nov. 2020) 115911, https://doi.org/10.1016/j.ces.2020.115911.
[110] B. Gielen, J. Jordens, L.C.J. Thomassen, L. Braeken, T. Van Gerven, Agglomeration control during ultrasonic crystallization of an active pharmaceutical ingredient, Crystals 7 (2) (2017) pp, https://doi.org/10.3390/cryst7020040.
[111] H. Ramirez Mendoza, J. Jordens, M. Valdez Lancinha Pereira, C. Lutz, T. Van Gerven, Effects of ultrasonic irradiation on crystallization kinetics, morphological and structural properties of zeolite FAU, Ultrason. Sonochem. 64 (Jun. 2020) 105010, https://doi.org/10.1016/j.ultsonch.2020.105010.
[112] Q. Zhao, L. Yang, C. Yao, G. Chen, Ultrasonic enhanced continuous crystallization: induction time and process control, Ind. Eng. Chem. Res. 62 (47) (Nov. 2023) 20083–20095, https://doi.org/10.1021/acs.iecr.3c02950.
[113] K. Kakinouchi, et al., Effect of ultrasonic irradiation on protein crystallization, J. Cryst. Growth 292 (2) (Jul. 2006) 437–440, https://doi.org/10.1016/j.jcrysgro.2006.04.051.
[114] S.G. Babu, et al., Synergistic effect of sono-photocatalytic process for the degradation of organic pollutants using CuO-TiO2/rGO, Ultrason. Sonochem. 50 (Jan. 2019) 218–223, https://doi.org/10.1016/j.ultsonch.2018.09.021.
[115] A. Hassani, M. Malhotra, A.V. Karim, S. Krishnan, P.V. Nidheesh, Recent progress on ultrasound-assisted electrochemical processes: A review on mechanism, reactor strategies, and applications for wastewater treatment, Environ. Res. 205 (Apr. 2022) 112463, https://doi.org/10.1016/j.envres.2021.112463.
[116] L. Borea, et al., Wastewater treatment by membrane ultrafiltration enhanced with ultrasound: effect of membrane flux and ultrasonic frequency, Ultrasonics 83 (Feb. 2018) 42–47, https://doi.org/10.1016/j.ultras.2017.06.013.
[117] M.J. Abeledo-Lameiro, E. Ares-Mazás, H. Goméz-Couso, Use of ultrasound irradiation to inactivate Cryptosporidium parvum oocysts in effluents from municipal wastewater treatment plants, Ultrason. Sonochem. 48 (Nov. 2018) 118–126, https://doi.org/10.1016/j.ultsonch.2018.05.013.
[118] P.M. Romero-Pareja, C.A. Aragon, J.M. Quiroga, M.D. Coello, Evaluation of a biological wastewater treatment system combining an OSA process with ultrasound for sludge reduction, Ultrason. Sonochem. 36 (May 2017) 336–342, https://doi.org/10.1016/j.ultsonch.2016.12.006.

[119] A. Al-Bsoul, et al., Optimal conditions for olive mill wastewater treatment using ultrasound and advanced oxidation processes, Scienceof the Total Environment 700 (Jan. 2020) 134576, https://doi.org/10.1016/j.scitotenv.2019.134576.
[120] N. Golash, P.R. Gogate, Degradation of dichlorvos containing wastewaters using sonochemical reactors, Ultrason. Sonochem. 19 (5) (Sep. 2012) 1051–1060, https://doi.org/10.1016/j.ultsonch.2012.02.011.
[121] B. Albero, J.L. Tadeo, R.A. Pérez, Ultrasound-assisted extraction of organic contaminants, TrAC Trends Anal. Chem. 118 (Sep. 2019) 739–750, https://doi.org/10.1016/j.trac.2019.07.007.
[122] F. Chemat, N. Rombaut, A.-G. Sicaire, A. Meullemiestre, A.-S. Fabiano-Tixier, M. Abert-Vian, Ultrasound assisted extraction of food and natural products. mechanisms, techniques, combinations, protocols and applications. a review, Ultrason. Sonochem. 34 (Jan. 2017) 540–560, https://doi.org/10.1016/j.ultsonch.2016.06.035.
[123] A. Altemimi, R. Choudhary, D.G. Watson, D.A. Lightfoot, Effects of ultrasonic treatments on the polyphenol and antioxidant content of spinach extracts, Ultrason. Sonochem. 24 (May 2015) 247–255, https://doi.org/10.1016/j.ultsonch.2014.10.023.
[124] J.J. John, S. Kuhn, L. Braeken, T. Van Gerven, Ultrasound assisted liquid–liquid extraction with a novel interval-contact reactor, Chemical Engineering and Processing: Process Intensification 113 (Mar. 2017) 35–41, https://doi.org/10.1016/j.cep.2016.09.008.
[125] D.-Y. Zhang, Y. Wan, J.-Y. Xu, G.-H. Wu, L. Li, X.-H. Yao, Ultrasound extraction of polysaccharides from mulberry leaves and their effect on enhancing antioxidant activity, Carbohydr. Polym. 137 (Feb. 2016) 473–479, https://doi.org/10.1016/j.carbpol.2015.11.016.
[126] P. Sharayei, E. Azarpazhooh, S. Zomorodi, H.S. Ramaswamy, Ultrasound assisted extraction of bioactive compounds from pomegranate (Punica granatum L.) peel, LWT 101 (Mar. 2019) 342–350, https://doi.org/10.1016/j.lwt.2018.11.031.
[127] G. Malietzis, et al., High-intensity focused ultrasound: advances in technology and experimental trials support enhanced utility of focused ultrasound surgery in oncology, BJR 86 (1024) (Apr. 2013) 20130044, https://doi.org/10.1259/bjr.20130044.
[128] F. Wu, et al., 'Wide local ablation' of localized breast cancer using high intensity focused ultrasound, J. Surg. Oncol. 96 (2) (Aug. 2007) 130–136, https://doi.org/10.1002/jso.20769.
[129] M.D. Gray, et al., Focused ultrasound hyperthermia for targeted drug release from thermosensitive liposomes: results from a phase I trial, Radiology 291 (1) (Apr. 2019) 232–238, https://doi.org/10.1148/radiol.2018181445.
[130] S. Kotopoulis, G. Dimcevski, O. Helge Gilja, D. Hoem, M. Postema, Treatment of human pancreatic cancer using combined ultrasound, microbubbles, and gemcitabine: a clinical case study, Med. Phys. 40 (7) (Jul. 2013) 072902, https://doi.org/10.1118/1.4808149.
[131] J. Liu, et al., Improving acute cardiac transplantation rejection therapy using ultrasound-targeted FK506-loaded microbubbles in rats, Biomater. Sci. 7 (9) (2019) 3729–3740.